In Silico Ascription of Gene Expression Differences to Tumor and Stromal Cells in a Model to Study Impact on Breast Cancer Outcome

Simen Myhre[1,2]*[9], Hayat Mohammed[1,3][9], Trine Tramm[4], Jan Alsner[4], Greg Finak[5], Morag Park[5], Jens Overgaard[4], Anne-Lise Børresen-Dale[1,2], Arnoldo Frigessi[3], Therese Sørlie[1,2]

1 Department of Genetics, Institute for Cancer Research, Division of Surgery and Cancer, Oslo University Hospital Radiumhospitalet, Oslo, Norway, **2** Institute of Clinical Medicine, Faculty of Medicine, University of Oslo, Oslo, Norway, **3** Department of Biostatistics, Institute of Basic Medical Sciences, University of Oslo, Oslo, Norway, **4** Department of Oncology, Aarhus University Hospital, Aarhus, Denmark, **5** Rosalind and Morris Goodman Cancer Centre, McGill University, Montreal, Canada

Abstract

Breast tumors consist of several different tissue components. Despite the heterogeneity, most gene expression analyses have traditionally been performed without prior microdissection of the tissue sample. Thus, the gene expression profiles obtained reflect the mRNA contribution from the various tissue components. We utilized histopathological estimations of area fractions of tumor and stromal tissue components in 198 fresh-frozen breast tumor tissue samples for a cell type-associated gene expression analysis associated with distant metastasis. Sets of differentially expressed gene-probes were identified in tumors from patients who developed distant metastasis compared with those who did not, by weighing the contribution from each tumor with the relative content of stromal and tumor epithelial cells in their individual tumor specimen. The analyses were performed under various assumptions of mRNA transcription level from tumor epithelial cells compared with stromal cells. A set of 30 differentially expressed gene-probes was ascribed solely to carcinoma cells. Furthermore, two sets of 38 and five differentially expressed gene-probes were mostly associated to tumor epithelial and stromal cells, respectively. Finally, a set of 26 differentially expressed gene-probes was identified independently of cell type focus. The differentially expressed genes were validated in independent gene expression data from a set of laser capture microdissected invasive ductal carcinomas. We present a method for identifying and ascribing differentially expressed genes to tumor epithelial and/or stromal cells, by utilizing pathologic information and weighted t-statistics. Although a transcriptional contribution from the stromal cell fraction is detectable in microarray experiments performed on bulk tumor, the gene expression differences between the distant metastasis and no distant metastasis group were mostly ascribed to the tumor epithelial cells of the primary breast tumors. However, the gene PIP5K2A was found significantly elevated in stroma cells in distant metastasis group, compared to stroma in no distant metastasis group. These findings were confirmed in gene expression data from the representative compartments from microdissected breast tissue. The method described was also found to be robust to different histopathological procedures.

Citation: Myhre S, Mohammed H, Tramm T, Alsner J, Finak G, et al. (2010) In Silico Ascription of Gene Expression Differences to Tumor and Stromal Cells in a Model to Study Impact on Breast Cancer Outcome. PLoS ONE 5(11): e14002. doi:10.1371/journal.pone.0014002

Editor: Hana Algül, Technische Universität München, Germany

Received April 13, 2010; **Accepted** October 26, 2010; **Published** November 19, 2010

Funding: This study was supported by the Norwegian Research Council (163027/V40 to TS and FUGE II, 175240/S10 to ALB), The Norwegian Cancer Society (PR-2006-0332 to TS and 80108003 to ALB), ''Foreningen for brystkreftoperterte'' (FFB), and the Centre Statistics for Innovation, The Danish Cancer Society, The Danish Medical Research Council and CIRRO - the Lundbeck Foundation Center for Interventional Research in Radiation Oncology, Réseau de Recherche en Cancer du FRSQ, and a Canadian Institutes of Health Research Team Grant to MP. The funders had no role in study design, data collection and analysis, decision to publish, or preparation of the manuscript.

Competing Interests: The authors have declared that no competing interests exist.

* E-mail: simenmy@rr-research.no

[9] These authors contributed equally to this work.

Introduction

Female breast cancer counts for over 465 000 deaths annually world wide (approximately 1.300.000 new cases), and is the most common cancer type among women [1]. Earlier diagnosis and more efficient treatment strategies have reduced the mortality and lowered the risk for recurrence. Established molecular markers such as the estrogen receptor (ER), progesterone receptor (PgR) and human epidermal growth factor receptor 2 (*HER2/neu*) are considered routinely for treatment decisions [2].

Whole-genome DNA microarrays for gene expression have made it possible to unravel biological mechanisms underlying the disease at the transcriptomic level [3]. Microarray experiments allow for measurements and comparisons of gene expression within a sample as well as between multiple samples. For example, gene expression profiling has shown that breast tumors can be classified into subgroups displaying distinct characteristics with respect to both clinical markers and patient outcome [4–7], which emphasizes that breast cancer is a heterogeneous disease that should be treated accordingly. Specific gene signatures have been identified that correlate with different aspects of the disease, including two risk-predictors for distant recurrence that are currently being tested in large clinical trials [8–12].

Breast carcinomas are heterogeneous "organs" with a microenvironment of various cell types both within the tumor area and in the surroundings. Lymphocytic infiltrations, fibrosis, angio- and lymphanogenesis, and stromal cells (including fibroblasts, myofibroblasts and adipocytes), leukocytes, and myoepithelial cells may influence the development and further progression of the carcinoma cells [13]. Although there are studies showing that alterations and involvement of the microenvironment (stromal tissue) of breast carcinomas influence outcome [14,15], most gene expression analyses have been performed using the bulk tumor, without further reference to the stromal content. Hence, without performing any cell selection (by microdissection) prior to gene expression analysis, the output data have contained transcriptomic information from all tissue components in the sample. The variable contribution from different cell fractions makes it difficult to state whether differences in gene expression between samples arise from distinct expression within the same cell type, and/or reflect the diversity in gene expression between various types of cells [16].

Cleator and colleagues [17] showed, using gene expression microarray analysis, that the stromal component of breast carcinomas influenced the prediction of therapy response. They emphasized the significant effect the non-tumor-cell content of breast cancer samples has on gene expression profiles. Furthermore, in a study of prostate cancer, Stuart and colleagues [18] linked, *in silico*, the relative content of tumor cells, benign hyperplastic epithelium, stroma, and dilated cystic glands in 88 prostate specimens to gene expression levels determined by microarray analysis. They were able to identify gene expression differences between non-malignant and malignant epithelial cells without being confounded by the gene expression of stromal cells. Since the content of tumor cells varies between patient samples, a threshold for minimum content of tumor cells within a sample is often applied. Such a threshold is quite arbitrary and would exclude potentially important cell type interactions.

In this study we utilized the histopathological information of tumor epithelial cell and stromal cell area-fractions to perform cell type-associated gene expression analyses of primary breast tumors. We compared a group of breast cancer patients who experienced distant metastasis (DM) with a group who experienced no distant metastasis (NoDM) during a median follow up period of >15 years. In this approach, using tumor epithelial cell-based weights, a sample where these cells cover a small percentage of the area of the tissue sample, will contribute less than a sample where tumor cells are more abundant when investigating gene expression differences originating in tumor tissue. We provide here an *in silico* method to ascribe differentially expressed gene-probes (DEGs) in primary breast tumors between patients experiencing DM and patients experiencing NoDM to either tumor epithelial and/or stroma cells.

Results and Discussion

Initially a standard t-test was performed, referred to as the "unweighted analysis", between the DM and NoDM tumor groups in a set of primary breast tumor samples from 198 patients. Clinical characteristics are given in Table 1. The un-weighted test identified 182 differentially expressed gene-probes (DEGs) at a 5% FDR level (Table S1"). This gene-probe list was in the following referred to as the *UWA-list* (Un-weighted analysis-list). Similar results were obtained when using variations of the t-statistics, as presented by Tusher and colleagues [19].

Table 1. Clinical information.

			DM		NoDM	
p- value	**Parameter**		**No.**	**%**	**No.**	**%**
	All		118	60	80	40
0.692	Protocol b	CMF	55	47	35	44
	Protocol c	TAM	63	53	45	56
0.105	Radiotherapy	YES	54	46	46	58
		NO	64	54	34	42
0,054	Tumor Sixe	<20 mm	32	27	30	38
		20–50 mm	64	54	44	55
		>50 mm	22	19	6	7
0.000	Pos lymph nodes	None	8	7	3	4
		1–3	43	36	62	77
		>3	67	57	15	19
0.002	Histopathology	Ductal	90	77	63	86
		Nonductal	28	23	17	14
0.004	Malignancy	Grade 1	17	19	17	27
	(Ductal-only)	Grade 2	42	47	39	62
		Grade 3	31	34	7	11
0.008	ER-status	Neg	39	33	13	16
		Pos	79	67	67	84
		Unknown	0	0	0	0

The null hypothesis is that the probabilities for each outcome (DM or noDM) are independent of the state or treatment (as written in the column).
One sided Chi-square or Fisher exact test for 2 by 2 or 2 by three contingency tables.
doi:10.1371/journal.pone.0014002.t001

Testing the relationship between cell area fraction and overall expression

For every tumor sample, histopathologic information regarding the content of different tissue components (tumor epithelium, stroma and adipocytes) was available (see Materials and methods).The distribution of the different tissue components was not significantly different (p-value 0.78 for tumor epithelial cells and 0.87 for stromal cells, Kolmogorov-Smirnov two-sample test) between the DM and noDM groups (Figure 1).

In order to test if the pathological numbers of the area fraction of tumor epithelial and stromal cells made an impact on the expression data we collected a list of genes reported to be stromal or tumor cell related in breast cancer by literature search [17,20]. Two methods were applied to see how the expression of these genes was related to the pathological numbers in our data. In the first approach, we compared gene expression data from the 15 tumor pieces having the highest stroma cell area-fraction with the expression data from the 15 tumor pieces having the highest tumor epithelial cell area-fraction. By doing a SAM [19] between the high tumor epithelial cell - and high stroma cell area fraction samples, we obtained one list of genes whose expression were elevated in the samples with high tumor epithelial cell area-fraction (list A), and one list of genes whose expression were elevated in the samples with high stroma cell area-fraction (list B). In the second approach we calculated the Pearson correlation between the gene expression for all genes and the mean centered pathological numbers for stromal (list C) and tumor epithelial cell area-fractions (list D) (across all 198 samples). The majority of the genes extracted from the literature were confirmed in our data,

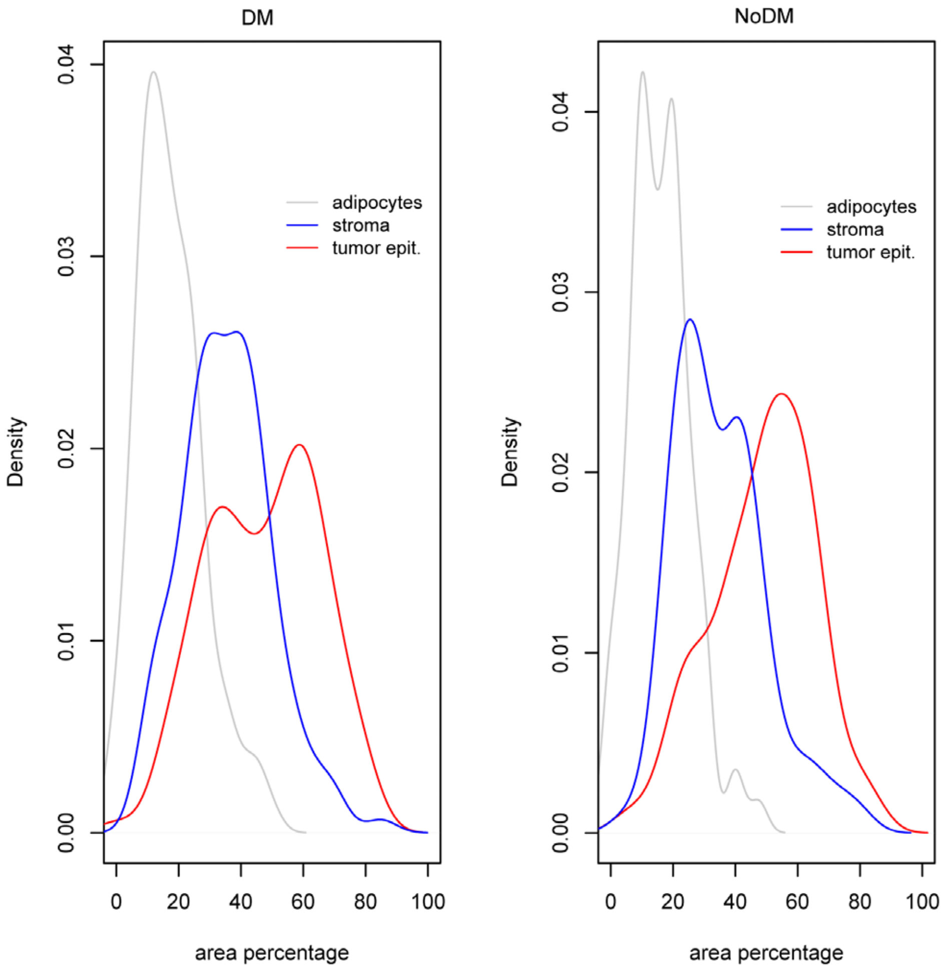

Figure 1. Cell type distribution between outcome groups. The density of the data was estimated by kernel smoothing where each point on the curve gives the probability (on the y-axis) of observing a given value x (of the x-axis). Percentages of the area of H&E sections of three different tissue components; tumor epithelial cells, stromal cells and adipocytes, grouped by clinical group. (DM = distant metastasis; NoDM = no distant metastasis).
doi:10.1371/journal.pone.0014002.g001

thus indicating that the pathological scoring of tissue components was robust (see Table S2). This indicates that both tumor stroma and tumor epithelial cells contribute a measurable amount of mRNA transcripts into the gross gene expression signal from the bulk tumor. We were not able to identify any candidate markers for adipocytic expression.

Robustness with respect to histopathology

The histopathological numbers utilized in the weighted analyses were crude estimates of area-fractions of tumor epithelial, stroma and adipocytic cells. In order to assess the robustness of the weighting approach in relation to the histopathological procedure, stereological point counting was performed additionally on a representative selection of the tissue sections. The numbers of area fraction from the stereological point counting were then utilized to calculate new weights for the sub-selection of samples. The new weights were compared to the initial weights used in the analyses. If the weights from the two methods were significantly different, then the output from the analyses would depend on the histopathological method applied. The first step of the validation was to test if the 109 samples selected for stereological point counting were representative for the whole set of 198 samples. None of the three statistical tests which compared the mean area-fraction for tumor epithelial, stroma and adipocytes respectively in the two sets of samples were found to be significant. Therefore we concluded that the 109 samples were representative for the whole data set. The second step was to compare the area-fraction numbers of tumor-epithelial, stroma and adipocytes in the 109 samples common for the two histopathological procedures. The differences in area fractions between the two procedures were highly significant for all three area fractions estimated. The stereological point counting tended to give a lower scoring of tumor epithelium and adipocytes and a higher scoring of stroma area-fraction, compared to the initial histopathological estimates. Hence, these tests revealed significant differences in the exact area fraction values measured with the two methods which are in accordance with previous publications determining that semi-quantitative measurements tend to produce an overestimation as compared to stereology [21]. However, in the weighted analyses it is not the proportion of tumor epithelial versus stroma cell area fraction within one sample that is important. But rather how the numbers of tumor epithelial and stroma area-fraction in the individual samples are in respect to the total number of tumor epithelial and respectively stroma area-fraction in all samples (in this case the group of individuals who did or did not experience DM). Therefore, new tumor and stroma weights were computed based on the number of area fraction from the stereological point counting. Then the weights were re-scaled by setting the level of transcription of adipocytes to null as described in the ''statistical methods'' section. The new weights were compared to the original ones in a paired t-test. The obtained p-values for the paired t-test were close to one for both the tumor and stroma weight comparisons, indicating no differences between the weights derived from the two histopathological approaches. Hence, it appears from these analyses that the weighting method is robust to variations in histopathological procedures.

Weighing under different assumptions of adipocyte transcription

The level of transcriptional contribution from adipocytes, compared to tumor epithelial and stromal cells in a heterogenous compartment is uncertain. Therefore, the statistical analyses were first carried out under various assumptions on the relative transcriptional efficiency of adipocytes compared to the two other tissue components. In the first series of analyses, DEGs between the DM and NoDM groups were identified under two different assumptions of mRNA levels in adipocytes (denoted by c): Firstly, we assumed that total adipocyte transcription level was equal to stroma cells and tumor epithelial cells ($c = 1$); secondly, we assumed no transcription in adipocytes ($c = 0$). The weighted analyses were divided into *tumor-focused analyses* (TFA) and *stroma-focused analyses* (SFA). In TFA, each sample was weighed proportionally to the area fraction tumor epithelium of that tumor sample, while in SFA, by the stromal cell percentage of that tumor sample. Thus, higher impact in the statistical analysis was given to samples containing more tumor epithelium or stromal cells, respectively. The TFA and the SFA respectively returned 169 and 77 DEGs, under the assumption of no transcription in adipocytes ($c = 0$). When the adipocyte transcription was weighed equally as for tumor epithelium and stroma ($c = 1$), the numbers of DEGs found between DM and NoDM tumor groups were 169 in the TFA and 85 in SFA, respectively (Figure 2). All the DEGs were obtained after multiple testing adjustments (5% FDR).

There were several overlapping gene-probes in the lists of DEGs. Fourty-five gene-probes were found in common between UWA and the lists from both weighted analyses (TFA and SFA) when $c = 0$. An identical number of overlapping probes between UWA and the weighted analyses were also identified under the assumption of $c = 1$ (Figure 2). The intersection of these two core sets of 45 gene-probes was 31. Hence, these 31 gene-probes were identified by the UWA as well as the SFA and TFA under both assumptions on adipocyte transcription ($c = 0$ and $c = 1$) and were among the most differentially expressed gene-probes between the two outcome groups. In addition, most of the 182 probes in UWA (representing 181 different genes) were also detected in the weighted analyses (141 for $c = 0$ and 138 for $c = 1$). The remaining probes (41 and 44 when $c = 0$ and $c = 1$, respectively) were not identified in the weighted analysis at 5% FDR but appeared as significant at 10 or 20% FDR. It is interesting that both the TFA and SFA identified probes that appeared as statistically non-significant in the standard un-weighted analysis. These were 48 and 55 tumor-associated probes (when $c = 0$, and $c = 1$, respectively) and 12 and 16 stroma-associated probes (for $c = 0$ and $c = 1$, respectively) (Figure 2).

Lists of DEGs identified through weighing by tumor epithelium and stroma content were then generated separately for other various assumptions of adipocyte transcription levels from $c = 0$ *to* 1 ($c = 0, 0.2, 0.4, 0.6, 0.8$ *and* 1). In summary, in the TFA there were 105 DEGs which appeared for all the selected adipocyte transcription levels (tumor associated consensus-list with adipocyte transcription, *TACat*) (Figure 3), while there were 38 DEGs in the stroma consensus list (stroma associated consensus with adipocyte transcription, *SACat*) (Figure 4). Based on these analyses and the comparison of all generated lists of DEGs under various assumptions of adipocyte transcription level, we decided to proceed the analyses with $c = 0$, as the impact on the differentially expressed gene-probes between DM and noDM under the various assumptions on adipocyte transcription was minor.

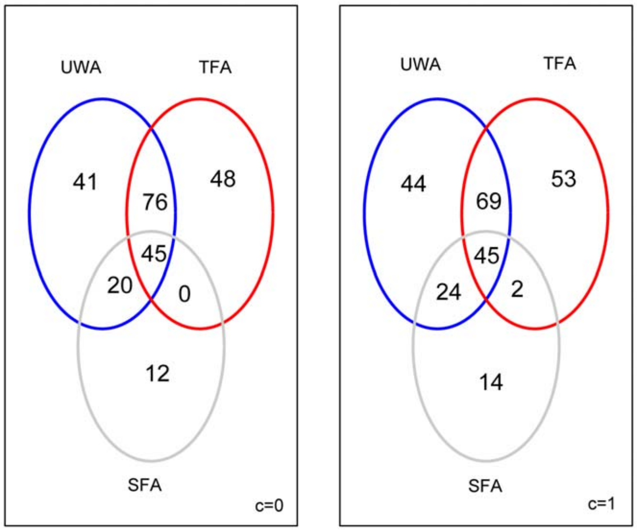

Figure 2. Overlap of differentially expressed gene-probes for different assumptions of adipocyte transcription. The Venn diagrams illustrate the sets of differentially expressed gene-probes with their intersections. The number of probes are given in each set, identified in unweighted (blue), tumor-focused (red) and stroma-focused (grey) analyses, respectively, when adipocytes contribute no transcript ($c = 0$), and when adipocytes contribute equally to tumor and stroma cells ($c = 1$).
doi:10.1371/journal.pone.0014002.g002

Weighing under different assumptions of stromal cell transcription

Even though the contribution from fat cells on transcriptional differences between two outcome groups in our analyses seems to be minimal, this may not be the case for stromal cells. In fact, it has been suggested that genes expressed in tumor-related stroma may predict disease outcome for breast cancer patients [15]. In the next series of analyses of differentially expressed gene-probes between tumors from patients experiencing DM or NoDM during follow up, we performed both tumor-epithelium-focused and stroma-focused analyses under various assumptions on mRNA level from the stromal compartment. Similarly to the above analyses, we varied the stromal expression strength d, in five intervals from 0.2 to 1 ($d = 0$ was not selected as it would be equivalent to the UWA), and identified five lists of DEGs in the tumor-weighted analysis (Figure 5). If the true stromal transcription level (compared with tumor epithelium) was known, the list of DEGs identified using the true d would be selected. Since the true d is unknown, these five lists were interpreted together. When $d = 1$, stromal and tumor epithelial cells were assumed to have equal levels of mRNA transcription. In the tumor-focused analyses, the contribution of each sample then equaled the samples' tumor epithelium percentage. For each selected value of d, the individual sample weights were re-scaled (see Materials and methods). A low value of d assumes low mRNA transcription level

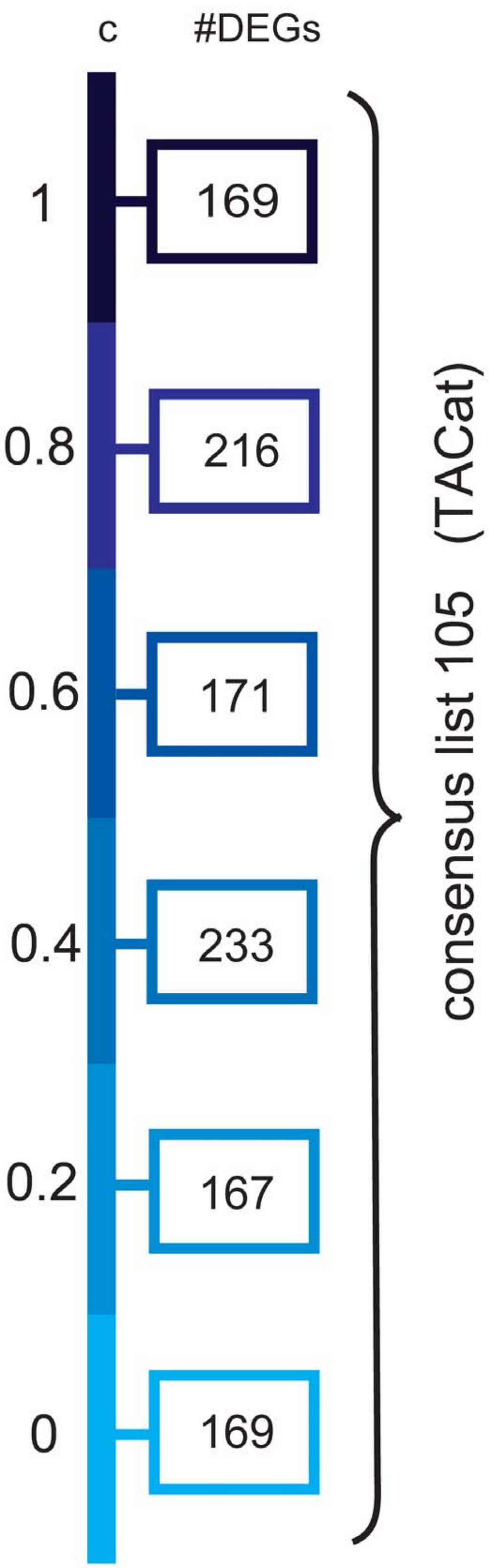

Tumor Focused Analyses

	Celera ID	Unigene ID	Symbol	Gene Name
🟩	hcg38221	Hs.282901	RNPC2	RNA-binding region (RNP1, RRM) containing 2
🟩	hcg32916	Hs.551518	RABEP1	rabaptin, RAB GTPase binding effector protein 1
🟥	hcg1811826	Hs.123253	SHCBP1	SHC SH2-domain binding protein 1
🟥	hcg27357	Hs.224152	TUBGCP3	tubulin, gamma complex associated protein 3
🟩	hcg25653	unknown	unknown	unknown
🟩	hcg41421	Hs.418533	BUB3	BUB3 budding uninhibited by benzimidazoles 3 homolog (yeast)
🟩	hcg2000584	Hs.134470	MSI2	musashi homolog 2 (Drosophila)
🟩	hcg21731	Hs.567295	ITPR1	inositol 1,4,5-triphosphate receptor, type 1
🟩	NM_002477	Hs.410970	MYL5	myosin, light polypeptide 5, regulatory
🟩	hcg28093	Hs.32973	GLRB	glycine receptor, beta
🟩	hcg2028477	Hs.414809	KIAA0831	KIAA0831
🟥	hcg1641210	Hs.388255	DC13	unknown
🟩	hcg42025	Hs.10846	SAT2	spermidine/spermine N1-acetyltransferase 2
🟩	hcg1991532	Hs.448851	USP6	ubiquitin specific peptidase 6 (Tre-2 oncogene)
🟩	hcg22120	Hs.509414	KTN1	kinectin 1 (kinesin receptor)|protein disulfide isomerase family A, member 6
🟩	hcg21575	Hs.501309	CIRBP	cold inducible RNA binding protein
🟩	hcg28572	Hs.550529	CARD14	caspase recruitment domain family, member 14
🟩	hcg1773669	Hs.443837	NPEPPS	aminopeptidase puromycin sensitive
🟩	hcg39942	Hs.519602	NME5	non-metastatic cells 5, protein expressed in (nucleoside-diphosphate kinase)
🟩	hcg27600	Hs.304249	UGCG	UDP-glucose ceramide glucosyltransferase
🟩	hcg17859	Hs.519346	ERBB2IP	erbb2 interacting protein
🟩	hcg38615	Hs.169333	TIGD6	tigger transposable element derived 6
🟩	hcg2033819	Hs.167165	FLJ12975	unknown
🟩	hcg172494	Hs.567748	FLJ90396	unknown
🟩	hcg32915	Hs.567613	RIP	unknown
🟩	hcg16958	Hs.12272	BECN1	beclin 1 (coiled-coil, myosin-like BCL2 interacting protein)
🟥	hcg33186	Hs.507162	VPS37B	vacuolar protein sorting 37B (yeast)
🟥	hcg2025279	Hs.518997	C1orf106	chromosome 1 open reading frame 106
🟩	hcg17158	Hs.131226	BNIP3L	BCL2/adenovirus E1B 19kDa interacting protein 3-like
🟩	hcg32982	Hs.461954	SRR	serine racemase
🟩	hcg39726	Hs.159799	THRAP2	thyroid hormone receptor associated protein 2
🟩	hcg25207	unknown	unknown	unknown
🟩	hcg2014575	Hs.168799	METTL3	methyltransferase like 3
🟥	hcg2007005	Hs.17936	C15orf39	chromosome 15 open reading frame 39
🟩	hcg2040694	unknown	unknown	unknown
🟩	hcg41797	Hs.103110	LOC150383	unknown
🟥	hcg1741622	Hs.25544	TMEM39B	transmembrane protein 39B
🟩	hcg22265	Hs.26403	GSTZ1	glutathione transferase zeta 1 (maleylacetoacetate isomerase)
🟩	hcg33207	Hs.513871	MGC32124	unknown
🟥	hcg32785	Hs.435166	LBR	lamin B receptor
🟥	hcg401268	Hs.473918	SLC37A1	solute carrier family 37 (glycerol-3-phosphate transporter), member 1
🟩	hcg27732	Hs.476448	FLNB	filamin B, beta (actin binding protein 278)
🟩	hcg2039549	Hs.534293	SERPINA3	serpin peptidase inhibitor, clade A (alpha-1 antiproteinase, antitrypsin), membe
🟥	hcg1641046	unknown	unknown	unknown
🟩	hcg1642286	Hs.154652	C8orf72	chromosome 8 open reading frame 72
🟩	hcg1811142	Hs.335239	ANKRD28	ankyrin repeat domain 28
🟩	hcg2005965	Hs.173524	LKAP	unknown
🟥	hcg1778228	Hs.475502	TMEM40	transmembrane protein 40
🟩	hcg2041406	Hs.569361	C14orf167	chromosome 14 open reading frame 167
🟩	hcg20875	Hs.274337	PRPF39	PRP39 pre-mRNA processing factor 39 homolog (yeast)
🟩	hcg27691	Hs.13313	CREBL2	cAMP responsive element binding protein-like 2
🟩	hcg40198	Hs.368855	GMPR2	guanosine monophosphate reductase 2
🟩	hcg40281	Hs.233160	STC2	stanniocalcin 2
🟩	hcg1644459	Hs.482976	LOC90355	unknown
🟩	hcg39815	Hs.11729	SLC27A2	solute carrier family 27 (fatty acid transporter), member 2
🟩	hcg33379	Hs.532795	COIL	coilin
🟩	hcg2039988	Hs.483329	KIAA1961	unknown
🟩	hcg19840	Hs.386453	PORCN	porcupine homolog (Drosophila)
🟥	hcg401238	Hs.439309	TMPRSS2	transmembrane protease, serine 2
🟩	hcg37211	Hs.99528	RAB31	RAB31, member RAS oncogene family
🟩	hcg172497	Hs.515154	FBXW9	F-box and WD-40 domain protein 9
🟩	hcg32498	Hs.279061	C17orf25	chromosome 17 open reading frame 25
🟥	hcg24286	Hs.532824	MAPRE2	microtubule-associated protein, RP/EB family, member 2
🟩	hcg18250	Hs.253305	SLA/LP	unknown
🟩	hcg28077	Hs.459070	ARNT2	aryl-hydrocarbon receptor nuclear translocator 2
🟥	hcg1785265	Hs.12211	SLC35C1	solute carrier family 35, member C1
🟥	hcg1776592	Hs.446574	TMSB10	thymosin, beta 10
🟩	hcg1821182	Hs.263600	ZNF20	zinc finger protein 20 (KOX 13)
🟩	hcg37816	Hs.19306	SIRT3	sirtuin (silent mating type information regulation 2 homolog) 3 (S. cerevisiae)
🟥	hcg16488	Hs.275675	KATNB1	katanin p80 (WD repeat containing) subunit B 1
🟩	hcg2004402	Hs.200943	NARG2	NMDA receptor regulated 2
🟩	hcg30690	Hs.168762	ULK2	unc-51-like kinase 2 (C. elegans)
🟥	hcg1811947	Hs.14745	C10orf9	chromosome 10 open reading frame 9
🟩	hcg29967	Hs.526665	ZNF627	zinc finger protein 627
🟥	hcg33395	Hs.280387	LRP8	low density lipoprotein receptor-related protein 8, apolipoprotein e receptor
🟩	hcg1798356	Hs.20573	MGC18216	unknown
🟩	hcg2004088	unknown	LOC440503	unknown
🟩	hcg42027	Hs.27475	FLJ32499	unknown
🟩	hcg1781685	Hs.81934	ACADSB	acyl-Coenzyme A dehydrogenase, short/branched chain
🟩	hcg1642576	unknown	unknown	unknown
🟩	hcg1811078	Hs.397465	HIPK2	homeodomain interacting protein kinase 2
🟩	hcg2007908	Hs.290347	LOC440916	unknown
🟩	hcg27295	Hs.42645	SLC16A6	solute carrier family 16 (monocarboxylic acid transporters), member 6
🟩	hcg2038724	Hs.441601	FLJ42957	unknown
🟩	hcg2000586	Hs.514356	unknown	unknown
🟩	hcg1984771	Hs.490371	unknown	unknown
🟩	hcg2023709	Hs.260041	NBLA04196	unknown
🟩	hcg2002898	Hs.532082	IL6ST	interleukin 6 signal transducer (gp130, oncostatin M receptor)
🟥	hcg16493	Hs.408702	FLJ13154	unknown
🟥	hcg20077	Hs.88297	STK17B	serine/threonine kinase 17b (apoptosis-inducing)
🟥	hcg39308	Hs.368402	C8orf55	chromosome 8 open reading frame 55
🟩	hcg38343	Hs.434289	NUDT12	nudix (nucleoside diphosphate linked moiety X)-type motif 12
🟩	hcg40430	Hs.567704	TTBK2	tau tubulin kinase 2
🟩	hcg28250	Hs.155956	NAT1	N-acetyltransferase 1 (arylamine N-acetyltransferase)
🟩	hcg1794564	Hs.567889	ANKRD30B	ankyrin repeat domain 30B
🟥	hcg1812757	Hs.567352	TXNRD1	thioredoxin reductase 1
🟩	hcg32860	Hs.260720	DNAJC12	DnaJ (Hsp40) homolog, subfamily C, member 12
🟩	hcg1817975	Hs.203634	GSTO2	glutathione S-transferase omega 2
🟩	hcg1784573	Hs.88417	SUSD3	sushi domain containing 3
🟩	hcg1811238	Hs.505104	KLHDC5	kelch domain containing 5
🟩	hcg1820468	Hs.164595	CDRT4	CMT1A duplicated region transcript 4
🟩	hcg1818271	Hs.525105	SLITRK6	SLIT and NTRK-like family, member 6
🟩	hcg21166	Hs.65735	LOC90835	unknown
🟩	hcg32380	Hs.531941	MYB	v-myb myeloblastosis viral oncogene homolog (avian)
🟩	hcg1642202	Hs.145402	IFT74	intraflagellar transport 74 homolog (Chlamydomonas)

Figure 3. Differentially expressed gene-probes identified in the tumor-focused analysis for various assumptions of adipocyte transcription. A set of DEGs was identified from each of six analyses for different assumptions of c. A consensus list of 105 probes was categorized. Red boxes: up in DM ; Green boxes: up in NoDM. (TACat - tumor associated consensus-list with adipocyte transcription).
doi:10.1371/journal.pone.0014002.g003

in stromal cells compared to tumor cells, and the weight of each sample was therefore increased in a TFA and decreased in a SFA. For different values of d, the re-scaling of the weights gives stronger impact to samples with a high stroma percentage in a TFA as d is selected from 1 towards 0.2, since a low d assumes that the mRNA transcription mainly comes from tumor epithelial cells. Hence, the list of gene-probes from the TFA when d = 1 is less likely to contain DEGs originating from stromal tissue than when d = 0.2, because samples that consisted of mostly tumor epithelial cells counted more in the TFA when d = 1. Finally, in order to distinguish DEGs most likely to originate from tumor epithelium, we need to subtract the DEGs identified in the TFA with the DEGs identified in the SFA.

A set of 94 DEGs (tumor associated consensus-list stroma expression varied, *TACsev*) was identified regardless of the assumption on the level of stroma cell transcription d (Figure 5). The *TACsev*-list is less likely to contain DEGs originating from the stromal compartment since it includes the DEGs identified with d = 1.

Further, in the stroma-weighted analysis, again under various assumptions on the level d of transcription from stromal cells, the number of DEGs varied as *d* was increased from 0.2 to 1. Here, a set of 31 DEGs (stroma associated consensus list stroma expression varied, *SACsev*) was always identified regardless of the assumption on the level of transcription of stromal cells (Figure 6). The SFA is less prone to identify DEGs originating from tumor epithelial cells,

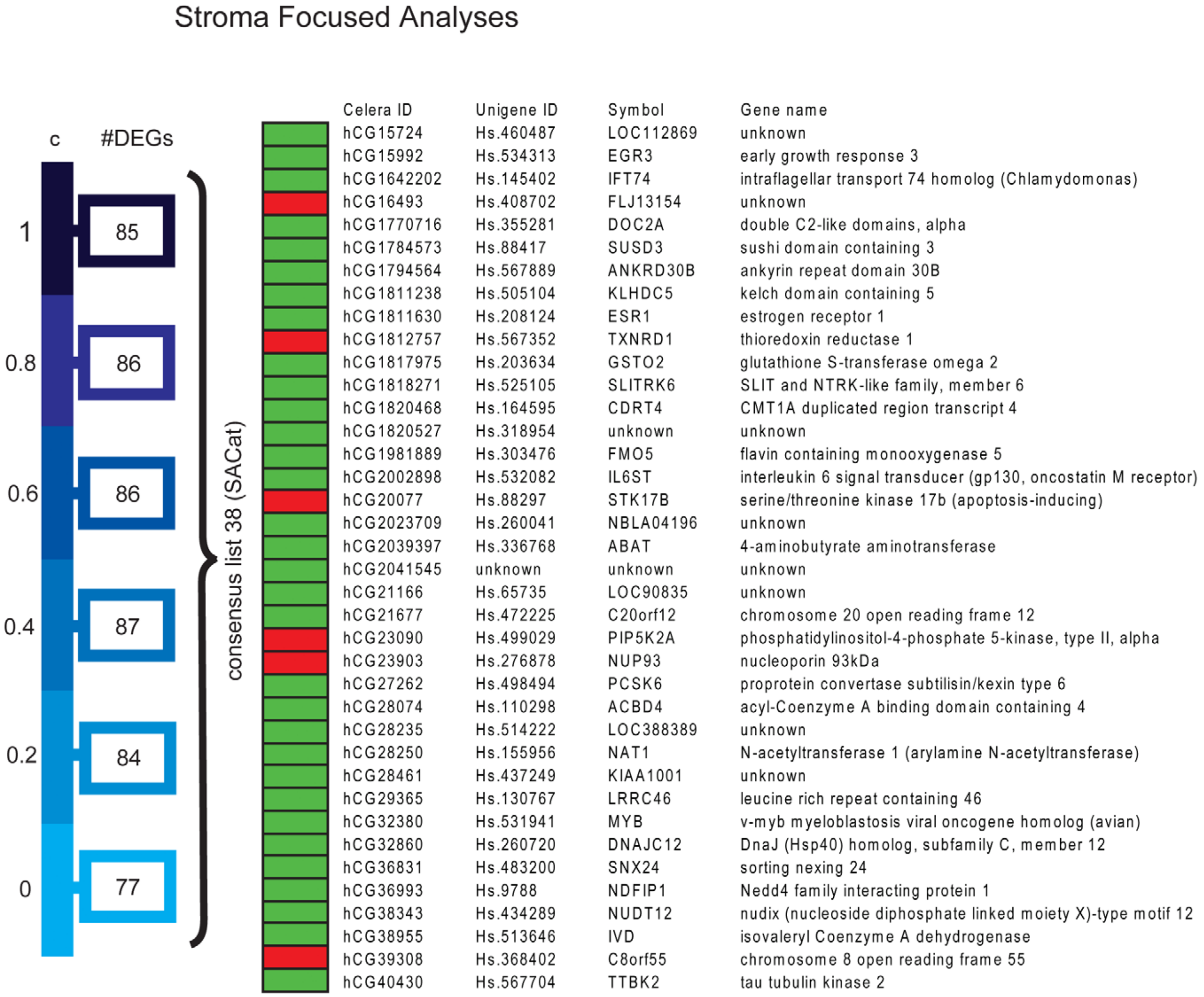

	Celera ID	Unigene ID	Symbol	Gene name
🟩	hCG15724	Hs.460487	LOC112869	unknown
🟩	hCG15992	Hs.534313	EGR3	early growth response 3
🟩	hCG1642202	Hs.145402	IFT74	intraflagellar transport 74 homolog (Chlamydomonas)
🟥	hCG16493	Hs.408702	FLJ13154	unknown
🟩	hCG1770716	Hs.355281	DOC2A	double C2-like domains, alpha
🟩	hCG1784573	Hs.88417	SUSD3	sushi domain containing 3
🟩	hCG1794564	Hs.567889	ANKRD30B	ankyrin repeat domain 30B
🟩	hCG1811238	Hs.505104	KLHDC5	kelch domain containing 5
🟩	hCG1811630	Hs.208124	ESR1	estrogen receptor 1
🟥	hCG1812757	Hs.567352	TXNRD1	thioredoxin reductase 1
🟩	hCG1817975	Hs.203634	GSTO2	glutathione S-transferase omega 2
🟩	hCG1818271	Hs.525105	SLITRK6	SLIT and NTRK-like family, member 6
🟩	hCG1820468	Hs.164595	CDRT4	CMT1A duplicated region transcript 4
🟩	hCG1820527	Hs.318954	unknown	unknown
🟩	hCG1981889	Hs.303476	FMO5	flavin containing monooxygenase 5
🟩	hCG2002898	Hs.532082	IL6ST	interleukin 6 signal transducer (gp130, oncostatin M receptor)
🟥	hCG20077	Hs.88297	STK17B	serine/threonine kinase 17b (apoptosis-inducing)
🟩	hCG2023709	Hs.260041	NBLA04196	unknown
🟩	hCG2039397	Hs.336768	ABAT	4-aminobutyrate aminotransferase
🟩	hCG2041545	unknown	unknown	unknown
🟩	hCG21166	Hs.65735	LOC90835	unknown
🟩	hCG21677	Hs.472225	C20orf12	chromosome 20 open reading frame 12
🟥	hCG23090	Hs.499029	PIP5K2A	phosphatidylinositol-4-phosphate 5-kinase, type II, alpha
🟥	hCG23903	Hs.276878	NUP93	nucleoporin 93kDa
🟩	hCG27262	Hs.498494	PCSK6	proprotein convertase subtilisin/kexin type 6
🟩	hCG28074	Hs.110298	ACBD4	acyl-Coenzyme A binding domain containing 4
🟩	hCG28235	Hs.514222	LOC388389	unknown
🟩	hCG28250	Hs.155956	NAT1	N-acetyltransferase 1 (arylamine N-acetyltransferase)
🟩	hCG28461	Hs.437249	KIAA1001	unknown
🟩	hCG29365	Hs.130767	LRRC46	leucine rich repeat containing 46
🟩	hCG32380	Hs.531941	MYB	v-myb myeloblastosis viral oncogene homolog (avian)
🟩	hCG32860	Hs.260720	DNAJC12	DnaJ (Hsp40) homolog, subfamily C, member 12
🟩	hCG36831	Hs.483200	SNX24	sorting nexing 24
🟩	hCG36993	Hs.9788	NDFIP1	Nedd4 family interacting protein 1
🟩	hCG38343	Hs.434289	NUDT12	nudix (nucleoside diphosphate linked moiety X)-type motif 12
🟩	hCG38955	Hs.513646	IVD	isovaleryl Coenzyme A dehydrogenase
🟥	hCG39308	Hs.368402	C8orf55	chromosome 8 open reading frame 55
🟩	hCG40430	Hs.567704	TTBK2	tau tubulin kinase 2

Figure 4. Differentially expressed gene-probes identified in the stroma-focused analysis for various assumptions of adipocyte transcription. In the stroma-focused analysis, a **set** of genes for each assumption of c was identified and a consensus list of 38 probes was determined. Red boxes: up in DM ; Green boxes: up in NoDM. (SACat - stroma associated consensus with adipocyte transcription).
doi:10.1371/journal.pone.0014002.g004

Tumor Focused Analyses

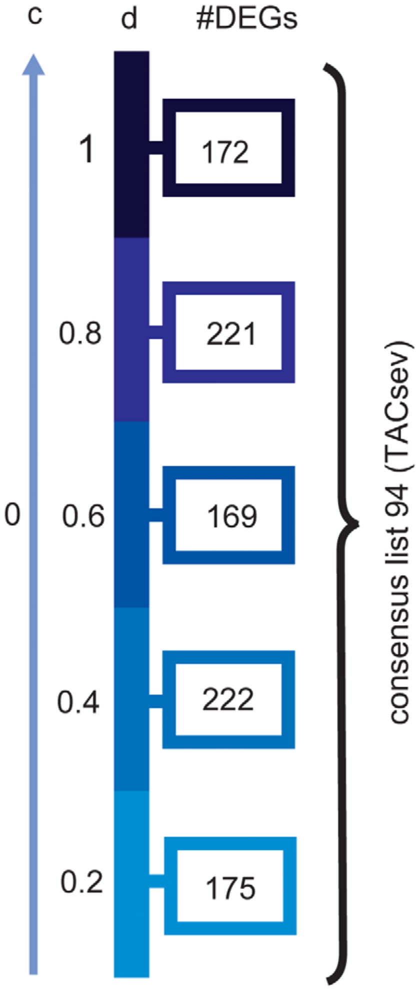

	Celera ID	Unigene ID	Symbol	Gene name
🟩	hCG38221	Hs.282901	RNPC2	RNA-binding region (RNP1, RRM) containing 2
🟩	hCG32916	Hs.551518	RABEP1	rabaptin, RAB GTPase binding effector protein 1
🟩	hCG2039616	Hs.171265	MDM1	Mdm4, transformed 3T3 cell double minute 1, p53 binding protein (mouse)
🟩	hCG15724	Hs.460487	LOC112869	unknown
🟩	hCG21046	Hs.480519	PLA2G12A	phospholipase A2, group XIIA
🟥	hCG27357	Hs.224152	TUBGCP3	tubulin, gamma complex associated protein 3
🟩	hCG2000584	Hs.134470	MSI2	musashi homolog 2 (Drosophila)
🟩	hCG2023709	Hs.260041	NBLA04196	unknown
🟩	NM_002477	Hs.410970	MYL5	myosin, light polypeptide 5, regulatory
🟩	hCG28093	Hs.32973	GLRB	glycine receptor, beta
🟥	hCG1732285	Hs.30868	RTN4R	reticulon 4 receptor
🟥	hCG1641210	Hs.388255	DC13	unknown
🟩	hCG2002898	Hs.532082	IL6ST	interleukin 6 signal transducer (gp130, oncostatin M receptor)
🟥	hCG16493	Hs.408702	FLJ13154	unknown
🟩	hCG37847	Hs.239154	ANKRA2	ankyrin repeat, family A (RFXANK-like), 2
🟩	hCG21575	Hs.501309	CIRBP	cold inducible RNA binding protein
🟥	hCG20077	Hs.88297	STK17B	serine/threonine kinase 17b (apoptosis-inducing)
🟩	hCG1773669	Hs.443837	NPEPPS	aminopeptidase puromycin sensitive
🟩	hCG39942	Hs.519602	NME5	non-metastatic cells 5, protein expressed in (nucleoside-diphosphate kinase)
🟩	hCG27600	Hs.304249	UGCG	UDP-glucose ceramide glucosyltransferase
🟩	hCG38615	Hs.169333	TIGD6	tigger transposable element derived 6
🟩	hCG2033819	Hs.167165	FLJ12975	unknown
🟩	hCG172494	Hs.567748	FLJ90396	unknown
🟩	hCG32915	Hs.567613	RIP	unknown
🟥	hCG2025279	Hs.518997	C1orf106	chromosome 1 open reading frame 106
🟩	hCG2024612	Hs.549236	TTC18	tetratricopeptide repeat domain 18
🟩	hCG38343	Hs.434289	NUDT12	nudix (nucleoside diphosphate linked moiety X)-type motif 12
🟩	hCG40430	Hs.567704	TTBK2	tau tubulin kinase 2
🟩	hCG25207	unknown	unknown	unknown
🟩	hCG1811630	Hs.208124	ESR1	estrogen receptor 1
🟥	hCG2007005	Hs.17936	C15orf39	chromosome 15 open reading frame 39
🟩	hCG28250	Hs.155956	NAT1	N-acetyltransferase 1 (arylamine N-acetyltransferase)
🟩	hCG1794564	Hs.567889	ANKRD30B	ankyrin repeat domain 30B
🟥	hCG1741622	unknown	unknown	unknown
🟩	hCG33207	Hs.513871	MGC32124	unknown
🟩	hCG17615	Hs.50282	RRAGB	Ras-related GTP binding B
🟥	hCG32785	Hs.435166	LBR	lamin B receptor
🟥	hCG401268	Hs.473918	SLC37A1	solute carrier family 37 (glycerol-3-phosphate transporter), member 1
🟩	hCG1640727	Hs.20573	IGF1R	insulin-like growth factor 1 receptor
🟥	hCG1812757	Hs.567352	TXNRD1	thioredoxin reductase 1
🟩	hCG32860	Hs.260720	DNAJC12	DnaJ (Hsp40) homolog, subfamily C, member 12
🟩	hCG1642286	Hs.154652	C8orf72	chromosome 8 open reading frame 72
🟩	hCG2039397	Hs.336768	ABAT	4-aminobutyrate aminotransferase
🟩	hCG1811142	Hs.335239	ANKRD28	ankyrin repeat domain 28
🟩	AK123974	Hs.410970	MYL5	myosin, light polypeptide 5, regulatory
🟩	hCG1817975	Hs.203634	GSTO2	glutathione S-transferase omega 2
🟩	hCG2041406	Hs.569361	C14orf167	chromosome 14 open reading frame 167
🟩	hCG28074	Hs.110298	ACBD4	acyl-Coenzyme A binding domain containing 4
🟩	hCG1784573	Hs.88417	SUSD3	sushi domain containing 3
🟩	hCG20875	Hs.274337	PRPF39	PRP39 pre-mRNA processing factor 39 homolog (yeast)
🟩	hCG27691	Hs.13313	CREBL2	cAMP responsive element binding protein-like 2
🟥	hCG28838	Hs.460988	CBFB	core-binding factor, beta subunit
🟩	hCG38240	Hs.22891	SLC7A8	solute carrier family 7 (cationic amino acid transporter, y+ system), member 8
🟩	hCG1820527	Hs.318954	unknown	unknown
🟩	hCG40198	Hs.368855	GMPR2	guanosine monophosphate reductase 2
🟩	hCG40281	Hs.233160	STC2	stanniocalcin 2
🟩	hCG1811238	Hs.505104	KLHDC5	kelch domain containing 5
🟩	hCG29192	Hs.133331	WDR31	WD repeat domain 31
🟩	hCG1820468	Hs.164595	CDRT4	CMT1A duplicated region transcript 4
🟩	hCG1644459	Hs.482976	LOC90355	unknown
🟩	hCG39815	Hs.11729	SLC27A2	solute carrier family 27 (fatty acid transporter), member 2
🟩	hCG1818271	Hs.525105	SLITRK6	SLIT and NTRK-like family, member 6
🟩	hCG37211	Hs.99528	RAB31	RAB31, member RAS oncogene family
🟩	hCG21166	Hs.65735	LOC90835	unknown
🟩	hCG172497	Hs.515154	FBXW9	F-box and WD-40 domain protein 9
🟥	hCG24286	Hs.532824	MAPRE2	microtubule-associated protein, RP/EB family, member 2
🟩	hCG32380	Hs.531941	MYB	v-myb myeloblastosis viral oncogene homolog (avian)
🟩	hCG18250	Hs.253305	SLA/LP	unknown
🟩	hCG1642202	Hs.145402	IFT74	intraflagellar transport 74 homolog (Chlamydomonas)
🟩	hCG28077	Hs.459070	ARNT2	aryl-hydrocarbon receptor nuclear translocator 2
🟥	hCG1776592	Hs.446574	TMSB10	thymosin, beta 10
🟩	hCG1821182	Hs.263600	ZNF20	zinc finger protein 20 (KOX 13)
🟩	hCG37816	Hs.19306	SIRT3	sirtuin (silent mating type information regulation 2 homolog) 3 (S. cerevisiae)
🟩	hCG17469	Hs.526735	ZMYND10	zinc finger, MYND-type containing 10
🟥	hCG16488	Hs.275675	KATNB1	katanin p80 (WD repeat containing) subunit B 1
🟩	hCG2004402	Hs.200943	NARG2	NMDA receptor regulated 2
🟩	hCG30690	Hs.168762	ULK2	unc-51-like kinase 2 (C. elegans)
🟥	hCG38475	Hs.344400	MPHOSPH6	M-phase phosphoprotein 6
🟥	hCG1811947	Hs.14745	C10orf9	chromosome 10 open reading frame 9
🟩	hCG29967	Hs.526665	ZNF627	zinc finger protein 627
🟥	hCG33395	Hs.280387	LRP8	low density lipoprotein receptor-related protein 8, apolipoprotein e receptor
🟩	hCG1798356	Hs.20573	MGC18216	unknown
🟩	hCG1811016	Hs.500812	BTRC	beta-transducin repeat containing
🟩	hCG2004088	unknown	LOC440503	unknown
🟥	hCG2030503	Hs.486401	C6orf173	chromosome 6 open reading frame 173
🟩	hCG42027	Hs.27475	FLJ32499	unknown
🟩	hCG1781685	Hs.81934	ACADSB	acyl-Coenzyme A dehydrogenase, short/branched chain
🟩	hCG1642576	unknown	unknown	unknown
🟥	hCG15060	unknown	unkown	unknown
🟩	hCG2007908	Hs.290347	LOC440916	unknown
🟩	hCG27295	Hs.42645	SLC16A6	solute carrier family 16 (monocarboxylic acid transporters), member 6
🟩	hCG2038724	Hs.441601	FLJ42957	unknown
🟩	hCG2000586	Hs.514356	unknown	unknown
🟩	hCG1984771	Hs.490371	unknown	unknown

Figure 5. Differentially expressed genes identified in the tumor-focused analysis for various assumptions of stroma transcription. Similarly, a set of DEGs was identified for each of six tumor-focused analyses, under various assumptions on the contribution of transcripts from stroma. A consensus list of 94 probes was determined. C = 0 for these analyses and the area of tumor and stroma cells was re-scaled to sum to 100. Red boxes: up in DM ; Green boxes: up in NoDM. (TACsev - tumor associated consensus-list stroma expression varied).
doi:10.1371/journal.pone.0014002.g005

since samples were weighted according to stroma content. In these analyses, a sample counted more if it consisted of more stroma (and hence less tumor cells) while it counted less if there were few stromal cells and proportionally more tumor epithelium, for each d from 1 to 0.2.

One of the values of d should be close to reflecting the true stromal contribution, but as this is unknown and *SACsev* represents the intersection of all the selected values of d, we expect most true DEGs to be in this list. These DEGs are likely to originate from stromal cells; if the same DEG also appears in *TAC*sev, it could be an indication that the tumor focused analyses wrongly ascribed the differential expression of this gene-probe to tumor cells. The DEGs in *TACsev* that are *not* in *SACsev* are hence more likely to be tumor epithelial cell-related. Because of these conceptual aspects, we focused on the identified DEGs that composed the intersections (consensus lists) from the analyses based on all 5 values of d *(TACsev* and *SACsev*), since these are most likely to withhold the true d (assuming the stroma transcription level was not less then <20% of tumor cell transcription level, as a conservative hypothesis) (Figure 7). We interpret these gene-probes as the most robustly identified DEGs between the DM and NoDM group, and the most biologically interesting. Finally, one important issue is that gene-probes whose expression profiles show extreme differences originating from tumor cells between the two outcome groups, might still have been identified in the stroma focused analyses even if tumor epithelium contributed less (and vice versa).

Biological interpretation of the consensus gene lists

We identified 68 DEGs in *TACsev* (94 DEG-list) that were not identified in *SACsev* (31 DEG-list). However, 38 of the 68 DEGs were identified by one or more of the stroma weighted analyses under different assumptions of stromal transcription level and could therefore not be ascribed exclusively to tumor epithelial cells (Figure 7). These 38 DEGs are therefore referred to as "tumor cells associated". We do propose that the differences in expression between DM and NoDM for the remaining 30 unique gene-probes in *TACsev* descended from tumor cells, since these were not identified by any of the five stroma weighted analyses. Among these were the insulin-like growth factor 1 receptor *(IGF1R)*, cAMP responsive element binding protein-like 2 *(CREBL2)*, and RAB31, member RAS oncogene family *(RAB31)*.

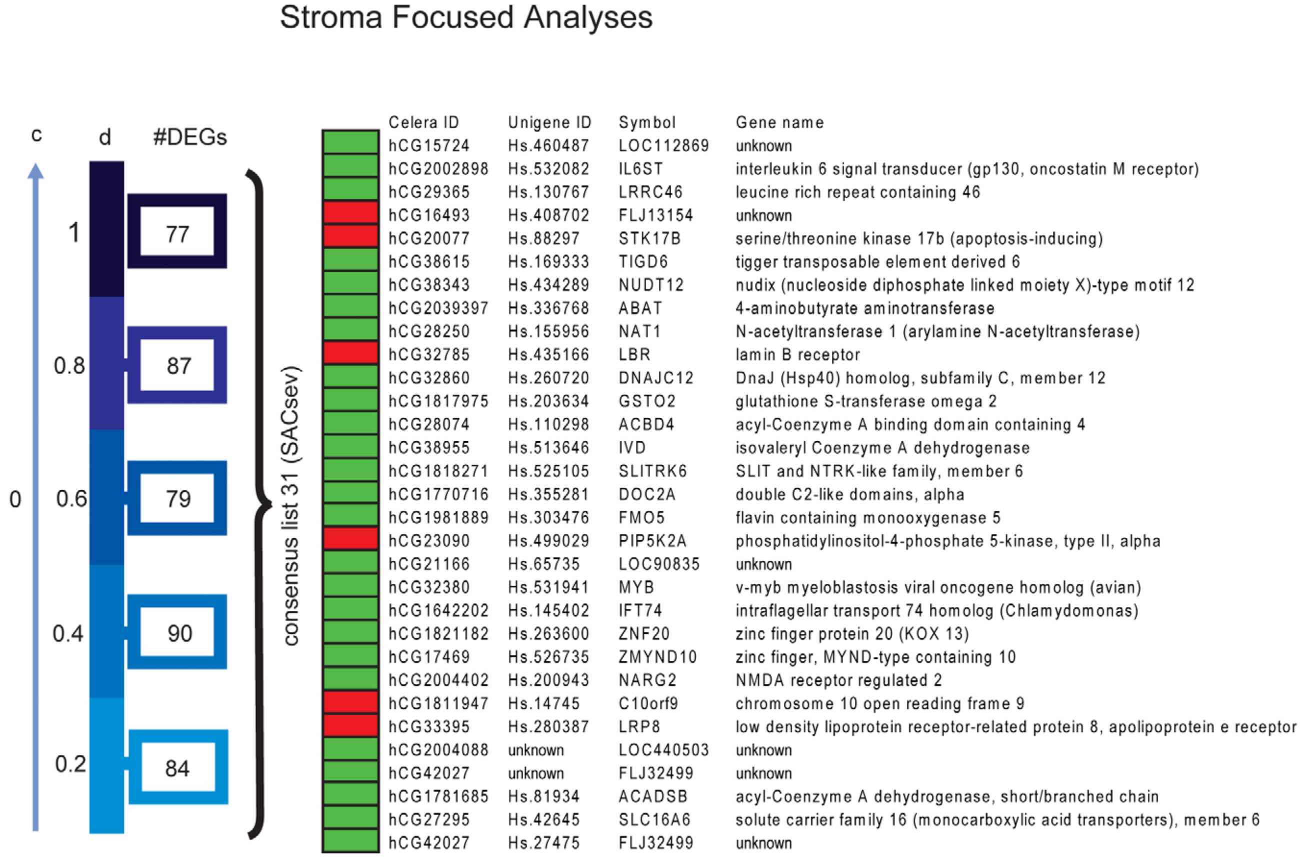

	Celera ID	Unigene ID	Symbol	Gene name
🟩	hCG15724	Hs.460487	LOC112869	unknown
🟩	hCG2002898	Hs.532082	IL6ST	interleukin 6 signal transducer (gp130, oncostatin M receptor)
🟩	hCG29365	Hs.130767	LRRC46	leucine rich repeat containing 46
🟥	hCG16493	Hs.408702	FLJ13154	unknown
🟥	hCG20077	Hs.88297	STK17B	serine/threonine kinase 17b (apoptosis-inducing)
🟩	hCG38615	Hs.169333	TIGD6	tigger transposable element derived 6
🟩	hCG38343	Hs.434289	NUDT12	nudix (nucleoside diphosphate linked moiety X)-type motif 12
🟩	hCG2039397	Hs.336768	ABAT	4-aminobutyrate aminotransferase
🟩	hCG28250	Hs.155956	NAT1	N-acetyltransferase 1 (arylamine N-acetyltransferase)
🟥	hCG32785	Hs.435166	LBR	lamin B receptor
🟩	hCG32860	Hs.260720	DNAJC12	DnaJ (Hsp40) homolog, subfamily C, member 12
🟩	hCG1817975	Hs.203634	GSTO2	glutathione S-transferase omega 2
🟩	hCG28074	Hs.110298	ACBD4	acyl-Coenzyme A binding domain containing 4
🟩	hCG38955	Hs.513646	IVD	isovaleryl Coenzyme A dehydrogenase
🟩	hCG1818271	Hs.525105	SLITRK6	SLIT and NTRK-like family, member 6
🟩	hCG1770716	Hs.355281	DOC2A	double C2-like domains, alpha
🟩	hCG1981889	Hs.303476	FMO5	flavin containing monooxygenase 5
🟥	hCG23090	Hs.499029	PIP5K2A	phosphatidylinositol-4-phosphate 5-kinase, type II, alpha
🟩	hCG21166	Hs.65735	LOC90835	unknown
🟩	hCG32380	Hs.531941	MYB	v-myb myeloblastosis viral oncogene homolog (avian)
🟩	hCG1642202	Hs.145402	IFT74	intraflagellar transport 74 homolog (Chlamydomonas)
🟩	hCG1821182	Hs.263600	ZNF20	zinc finger protein 20 (KOX 13)
🟩	hCG17469	Hs.526735	ZMYND10	zinc finger, MYND-type containing 10
🟩	hCG2004402	Hs.200943	NARG2	NMDA receptor regulated 2
🟥	hCG1811947	Hs.14745	C10orf9	chromosome 10 open reading frame 9
🟥	hCG33395	Hs.280387	LRP8	low density lipoprotein receptor-related protein 8, apolipoprotein e receptor
🟩	hCG2004088	unknown	LOC440503	unknown
🟩	hCG42027	unknown	FLJ32499	unknown
🟩	hCG1781685	Hs.81934	ACADSB	acyl-Coenzyme A dehydrogenase, short/branched chain
🟩	hCG27295	Hs.42645	SLC16A6	solute carrier family 16 (monocarboxylic acid transporters), member 6
🟩	hCG42027	Hs.27475	FLJ32499	unknown

Figure 6. Differentially expressed gene-probes identified in the stroma-focused analysis for various assumptions of stroma transcription. For various assumptions on stromal cell contribution, a set of DEGs was identified. C = 0 for these analyses and the area of tumor and stroma cells was re-scaled to sum to 100. A consensus list of 31 probes was determined. Red boxes: up in DM ; Green boxes: up in NoDM. (SACsev - stroma associated consensus list stroma expression varied).
doi:10.1371/journal.pone.0014002.g006

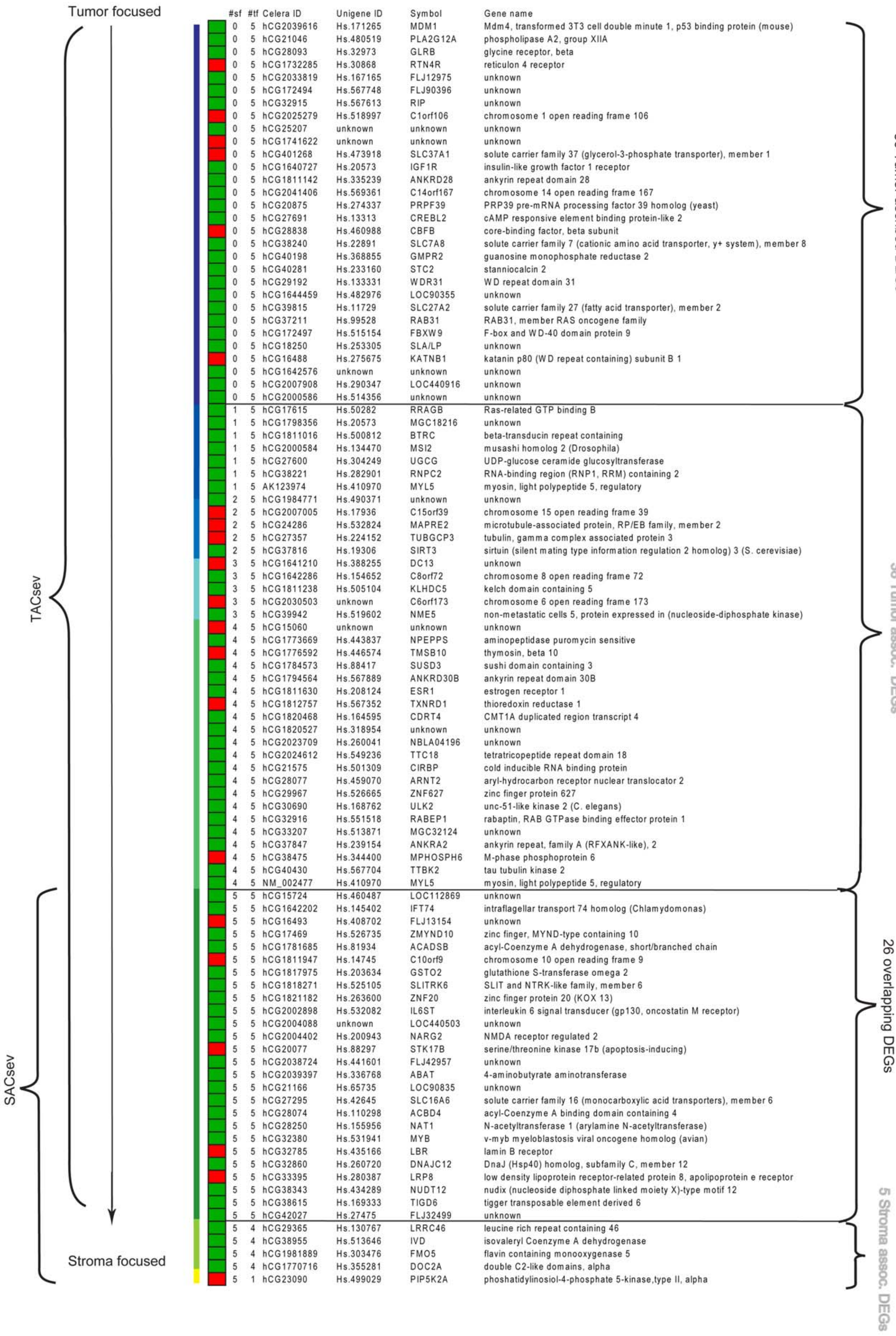
Tumor focused
TACsev
SACsev
Stroma focused
30 Tumor ascribed DEGs
38 Tumor assoc. DEGs
26 overlapping DEGs
5 Stroma assoc. DEGs

	#sf	#tf	Celera ID	Unigene ID	Symbol	Gene name
🟩	0	5	hCG2039616	Hs.171265	MDM1	Mdm4, transformed 3T3 cell double minute 1, p53 binding protein (mouse)
🟩	0	5	hCG21046	Hs.480519	PLA2G12A	phospholipase A2, group XIIA
🟩	0	5	hCG28093	Hs.32973	GLRB	glycine receptor, beta
🟥	0	5	hCG1732285	Hs.30868	RTN4R	reticulon 4 receptor
🟩	0	5	hCG2033819	Hs.167165	FLJ12975	unknown
🟩	0	5	hCG172494	Hs.567748	FLJ90396	unknown
🟩	0	5	hCG32915	Hs.567613	RIP	unknown
🟥	0	5	hCG2025279	Hs.518997	C1orf106	chromosome 1 open reading frame 106
🟩	0	5	hCG25207	unknown	unknown	unknown
🟥	0	5	hCG1741622	unknown	unknown	unknown
🟥	0	5	hCG401268	Hs.473918	SLC37A1	solute carrier family 37 (glycerol-3-phosphate transporter), member 1
🟩	0	5	hCG1640727	Hs.20573	IGF1R	insulin-like growth factor 1 receptor
🟩	0	5	hCG1811142	Hs.335239	ANKRD28	ankyrin repeat domain 28
🟩	0	5	hCG2041406	Hs.569361	C14orf167	chromosome 14 open reading frame 167
🟩	0	5	hCG20875	Hs.274337	PRPF39	PRP39 pre-mRNA processing factor 39 homolog (yeast)
🟩	0	5	hCG27691	Hs.13313	CREBL2	cAMP responsive element binding protein-like 2
🟥	0	5	hCG28838	Hs.460988	CBFB	core-binding factor, beta subunit
🟩	0	5	hCG38240	Hs.22891	SLC7A8	solute carrier family 7 (cationic amino acid transporter, y+ system), member 8
🟩	0	5	hCG40198	Hs.368855	GMPR2	guanosine monophosphate reductase 2
🟩	0	5	hCG40281	Hs.233160	STC2	stanniocalcin 2
🟩	0	5	hCG29192	Hs.133331	WDR31	WD repeat domain 31
🟩	0	5	hCG1644459	Hs.482976	LOC90355	unknown
🟩	0	5	hCG39815	Hs.11729	SLC27A2	solute carrier family 27 (fatty acid transporter), member 2
🟩	0	5	hCG37211	Hs.99528	RAB31	RAB31, member RAS oncogene family
🟩	0	5	hCG172497	Hs.515154	FBXW9	F-box and WD-40 domain protein 9
🟩	0	5	hCG18250	Hs.253305	SLA/LP	unknown
🟥	0	5	hCG16488	Hs.275675	KATNB1	katanin p80 (WD repeat containing) subunit B 1
🟩	0	5	hCG1642576	unknown	unknown	unknown
🟩	0	5	hCG2007908	Hs.290347	LOC440916	unknown
🟩	0	5	hCG2000586	Hs.514356	unknown	unknown
🟩	1	5	hCG17615	Hs.50282	RRAGB	Ras-related GTP binding B
🟩	1	5	hCG1798356	Hs.20573	MGC18216	unknown
🟩	1	5	hCG1811016	Hs.500812	BTRC	beta-transducin repeat containing
🟩	1	5	hCG2000584	Hs.134470	MSI2	musashi homolog 2 (Drosophila)
🟩	1	5	hCG27600	Hs.304249	UGCG	UDP-glucose ceramide glucosyltransferase
🟩	1	5	hCG38221	Hs.282901	RNPC2	RNA-binding region (RNP1, RRM) containing 2
🟩	1	5	AK123974	Hs.410970	MYL5	myosin, light polypeptide 5, regulatory
🟩	2	5	hCG1984771	Hs.490371	unknown	unknown
🟥	2	5	hCG2007005	Hs.17936	C15orf39	chromosome 15 open reading frame 39
🟥	2	5	hCG24286	Hs.532824	MAPRE2	microtubule-associated protein, RP/EB family, member 2
🟥	2	5	hCG27357	Hs.224152	TUBGCP3	tubulin, gamma complex associated protein 3
🟩	2	5	hCG37816	Hs.19306	SIRT3	sirtuin (silent mating type information regulation 2 homolog) 3 (S. cerevisiae)
🟥	3	5	hCG1641210	Hs.388255	DC13	unknown
🟩	3	5	hCG1642286	Hs.154652	C8orf72	chromosome 8 open reading frame 72
🟩	3	5	hCG1811238	Hs.505104	KLHDC5	kelch domain containing 5
🟥	3	5	hCG2030503	unknown	C6orf173	chromosome 6 open reading frame 173
🟩	3	5	hCG39942	Hs.519602	NME5	non-metastatic cells 5, protein expressed in (nucleoside-diphosphate kinase)
🟥	4	5	hCG15060	unknown	unknown	unknown
🟩	4	5	hCG1773669	Hs.443837	NPEPPS	aminopeptidase puromycin sensitive
🟥	4	5	hCG1776592	Hs.446574	TMSB10	thymosin, beta 10
🟩	4	5	hCG1784573	Hs.88417	SUSD3	sushi domain containing 3
🟩	4	5	hCG1794564	Hs.567889	ANKRD30B	ankyrin repeat domain 30B
🟩	4	5	hCG1811630	Hs.208124	ESR1	estrogen receptor 1
🟥	4	5	hCG1812757	Hs.567352	TXNRD1	thioredoxin reductase 1
🟩	4	5	hCG1820468	Hs.164595	CDRT4	CMT1A duplicated region transcript 4
🟩	4	5	hCG1820527	Hs.318954	unknown	unknown
🟩	4	5	hCG2023709	Hs.260041	NBLA04196	unknown
🟩	4	5	hCG2024612	Hs.549236	TTC18	tetratricopeptide repeat domain 18
🟩	4	5	hCG21575	Hs.501309	CIRBP	cold inducible RNA binding protein
🟩	4	5	hCG28077	Hs.459070	ARNT2	aryl-hydrocarbon receptor nuclear translocator 2
🟩	4	5	hCG29967	Hs.526665	ZNF627	zinc finger protein 627
🟩	4	5	hCG30690	Hs.168762	ULK2	unc-51-like kinase 2 (C. elegans)
🟩	4	5	hCG32916	Hs.551518	RABEP1	rabaptin, RAB GTPase binding effector protein 1
🟩	4	5	hCG33207	Hs.513871	MGC32124	unknown
🟩	4	5	hCG37847	Hs.239154	ANKRA2	ankyrin repeat, family A (RFXANK-like), 2
🟥	4	5	hCG38475	Hs.344400	MPHOSPH6	M-phase phosphoprotein 6
🟩	4	5	hCG40430	Hs.567704	TTBK2	tau tubulin kinase 2
🟩	4	5	NM_002477	Hs.410970	MYL5	myosin, light polypeptide 5, regulatory
🟩	5	5	hCG15724	Hs.460487	LOC112869	unknown
🟩	5	5	hCG1642202	Hs.145402	IFT74	intraflagellar transport 74 homolog (Chlamydomonas)
🟥	5	5	hCG16493	Hs.408702	FLJ13154	unknown
🟩	5	5	hCG17469	Hs.526735	ZMYND10	zinc finger, MYND-type containing 10
🟩	5	5	hCG1781685	Hs.81934	ACADSB	acyl-Coenzyme A dehydrogenase, short/branched chain
🟥	5	5	hCG1811947	Hs.14745	C10orf9	chromosome 10 open reading frame 9
🟩	5	5	hCG1817975	Hs.203634	GSTO2	glutathione S-transferase omega 2
🟩	5	5	hCG1818271	Hs.525105	SLITRK6	SLIT and NTRK-like family, member 6
🟩	5	5	hCG1821182	Hs.263600	ZNF20	zinc finger protein 20 (KOX 13)
🟩	5	5	hCG2002898	Hs.532082	IL6ST	interleukin 6 signal transducer (gp130, oncostatin M receptor)
🟩	5	5	hCG2004088	unknown	LOC440503	unknown
🟩	5	5	hCG2004402	Hs.200943	NARG2	NMDA receptor regulated 2
🟥	5	5	hCG20077	Hs.88297	STK17B	serine/threonine kinase 17b (apoptosis-inducing)
🟩	5	5	hCG2038724	Hs.441601	FLJ42957	unknown
🟩	5	5	hCG2039397	Hs.336768	ABAT	4-aminobutyrate aminotransferase
🟩	5	5	hCG21166	Hs.65735	LOC90835	unknown
🟩	5	5	hCG27295	Hs.42645	SLC16A6	solute carrier family 16 (monocarboxylic acid transporters), member 6
🟩	5	5	hCG28074	Hs.110298	ACBD4	acyl-Coenzyme A binding domain containing 4
🟩	5	5	hCG28250	Hs.155956	NAT1	N-acetyltransferase 1 (arylamine N-acetyltransferase)
🟩	5	5	hCG32380	Hs.531941	MYB	v-myb myeloblastosis viral oncogene homolog (avian)
🟥	5	5	hCG32785	Hs.435166	LBR	lamin B receptor
🟩	5	5	hCG32860	Hs.260720	DNAJC12	DnaJ (Hsp40) homolog, subfamily C, member 12
🟥	5	5	hCG33395	Hs.280387	LRP8	low density lipoprotein receptor-related protein 8, apolipoprotein e receptor
🟩	5	5	hCG38343	Hs.434289	NUDT12	nudix (nucleoside diphosphate linked moiety X)-type motif 12
🟩	5	5	hCG38615	Hs.169333	TIGD6	tigger transposable element derived 6
🟩	5	5	hCG42027	Hs.27475	FLJ32499	unknown
🟩	5	4	hCG29365	Hs.130767	LRRC46	leucine rich repeat containing 46
🟩	5	4	hCG38955	Hs.513646	IVD	isovaleryl Coenzyme A dehydrogenase
🟩	5	4	hCG1981889	Hs.303476	FMO5	flavin containing monooxygenase 5
🟩	5	4	hCG1770716	Hs.355281	DOC2A	double C2-like domains, alpha
🟥	5	1	hCG23090	Hs.499029	PIP5K2A	phoshatidylinosiol-4-phosphate 5-kinase,type II, alpha

Figure 7. Differentially expressed genes in TACsev and SACsev identified by the weighted analyses. The most repeatedly identified probes in either every tumor focused analysis or every stroma focused analysis for different values of d (assumed stromal transcription level). The '#tf' and '#sf' columns list in how many tumor focused and stroma focused analyses, respectively, the corresponding DEGs were identified. The colored vertical bar goes from darker blue (highly tumor associated) to lighter blue as the DEGs are identified in more stroma focused analyses (for different values of d), to green for DEGS found in both SFA and TFA, and finally yellow for stroma associated DEGs identified in fewer tumor focused analyses. Red boxes: up in DM ; Green boxes: up in NoDM.
doi:10.1371/journal.pone.0014002.g007

In the *SACsev* list we could not ascribe any DEGs purely to stroma cells since there were no DEGs between DM and NoDM that were not identified in at least one of the tumor-focused analyses (i.e. *TACsev*). In fact, four out of five SACsev gene probes not found in TACsev were still identified by four out of five tumor focused analyses when the contribution of stroma expression was varied (Figure 7). The fifth gene, phosphatidylinositol-4-phosphate 5-kinase, type II, alpha (*PIP5K2A*) was only identified by one of the five *TACsev*-analyses. These DEGs are therefore referred to as "stroma cells associated". However, it is interesting to note that these genes were identified by the tumor focused analyses for the lower values of d, hence, differences in gene expression from these five genes, and *PIP5K2A* in particular, might mainly be associated to stromal cells. *PIP5K2A* is part of the v-akt murine thymoma viral oncogene homolog 1 (*AKT1*) signaling pathway [22] and was higher expressed in tumors from patients who experienced distant metastasis. *PIP5K2A* has been reported to be involved in differentiation and motility; hence it might influence the metastatic process. The remaining four DEGs of the *SACsev* list that were not in *TACsev* were flavin containing monooxygenase 5 (*FMO5*), isovaleryl Coenzyme A dehydrogenase *(IVD)*, leucine rich repeat containing 46 *(LRRC46)*, and double C2-like domains, alpha *(DOC2A)*, all found to be lower expressed in the DM group. Longer relapse-free survival has previously been reported for patients with higher expression of *FMO5* [23] which is in line with the observed expression of *FMO5* in our study. Isovaleryl-CoA dehydrogenase (*IVD*) is a mitochondrial matrix enzyme that catalyzes the third step in leucine catabolism, and was found to be lower expressed in rats injected with estradiol valerate [24], which might indicate that this gene is downregulated by estrogen. In our study, *IVD*-expression was lower in the DM-group, in which tumors also showed lower expression of estrogen receptor 1 (*ESR1*) when compared to the NoDM group. It is on the other hand, questionable how comparable these two studies are. Regarding *LRRC46*, a recent study reports that this gene was expressed higher in estrogen receptor positive breast cancer tumors which are comparable to what was observed in our study [25]. *DOC2A* was reported to be highly expressed in brain cells where the protein was found to interact with Ca2+ and phospolipid in neurotransmission [26], and to our knowledge, no apparent connection between this gene and metastasis in breast cancer has previously been reported. There were two different *DOC2A*-probes present on the microarray used in this study, and only one of these showed significant difference in expression between the DM and NoDM groups. These probes might represent different splice variants, and need to be further validated.

There were 26 DEGs in common between the two consensus lists of DEGs (*TACsev*, and *SACsev*) (Figure 7). We consider these probes most robust in being differentially expressed between DM and NoDM since they are identified in every instance of cell type focus under different assumptions of stroma transcription. Among these 26 probes we did find known breast cancer related genes such as Arylamine N-acetyltransferase-1, (*NAT1*) [27], and v-myb myeloblastosis viral oncogene homolog (*MYB*), both reported earlier as a potential prognostic markers in estrogen receptor positive breast tumors [28]. Both *NAT1* and *MYB* were found to be lower expressed in the DM group in our data. Another gene of interest (also lower expressed in DM) is the zinc finger, MYND-type containing 10 (*ZMYND10*) gene, which has been suggested to act as a tumor suppressor gene in nasopharyngeal carcinomas [29]. All 26 DEGs in common between *TACsev and SACsev* lists were also found by the UWA. This is as expected since the criteria of the 26 gene list is that the DEGs were identified by all values of d in both TFA and SFA, also including the TFA with d = 0,2, a test being close to the UWA. Thus, the expression differences between the DM and NoDM groups for these probes seem to be sufficient to overshadow the weighing by either cell type. Conceptually, the cell type ascription of these DEGs could be explained by different scenarios; a) ascribed to tumor epithelial cells assuming the expression of tumor epithelial cells overshadows any effect of stroma; b), ascribed to stromal cells by assuming the expression differences in stroma were adequately profound to be detectable in a stroma focused analysis at low values of d (stroma-weighted test with d = 0,2) or c) these genes are differentially expressed between DM and NoDM in both cell type compartments. Analysis of expression differences for these genes in the validation data set indicates that a) is the most likely scenario of the three. However, we did validate one gene (ABAT) that was significantly differentially expressed between DM and NoDM in both tumor epithelial and tumor stroma.

Overlap between weighted and un-weighted tests

A total of five probes were identified in the consensus lists from the weighted analyses that were not among the DEGs from the un-weighted statistics (Figure 8). One probe from *SACsev* list (*PIP5K2A*), and 4 probes from the *TACsev* list (*FLJ90396*, *PRPF39*, *Unassigned* with homology to *Rab22*, and *MAPRE2*). *MAPRE2* (microtubule-associated protein, RP/EB family member 2) was found highly expressed in the DM group, and has been suggested (due to homology) to be involved in tumorigenesis of colorectal cancers and proliferation control in normal cells [30]. There is no reported function for the remaining three genes. Furthermore, we identified 88 probes (representing 88 genes) in UWA which were neither in *TACsev* nor *SACsev*. However, when we considered all 312 DEGs identified in the weighted analyses for all values of *d* between 0,2 - 1, there were 137 genes that were not present in the 182 UWA-list, and conversely, only 6 probes (6 genes) in the UWA list that were not present in any list from the weighted analyses (see Table S3).

Validation

In order to validate the tumor stromal and tumor epithelial ascribed (and associated) gene expression differences between the DM and NoDM groups, the expression of the genes in the consensus gene list (Figure 7) was tested in an independent data set. In the validation set, tumor epithelial cells and tumor stroma cells from 50 and 61 breast cancer patients, respectively, were isolated using laser capture microdissection (LCM) [15].

To assess the differences in expression of each gene between the DM and NoDM group a simple t-test was utilized. Out of the 30 tumor ascribed DEGs (in figure 7) 21 had available gene expression in the tumor-epithelial LCM validation set. Seven out

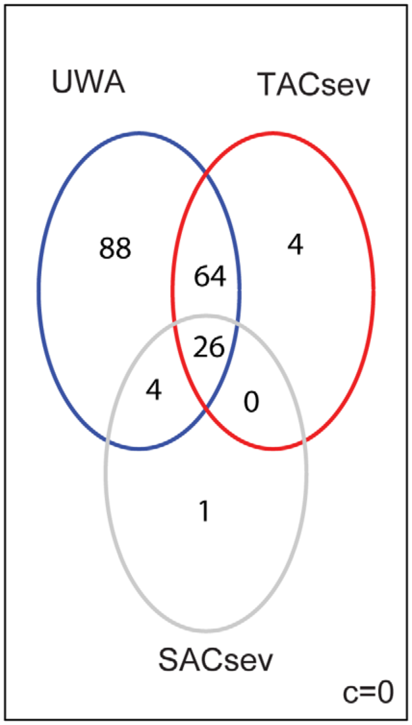

Figure 8. Overlap of differentially expressed gene-probes for the consensus lists (SACsev and TACsev) and UWA. The overlap of probes identified by the unweighted analysis and the intersection of all tumor weighted analyses and stroma weighted analyses with values of d from 1 to 0.2, under the assumption of no transcription in adipocytes. The majority of genes, 64 of the 68 tumor cell ascribed (30) and associated (38), and four of the five stromal cell associated are identified in the UWA.
doi:10.1371/journal.pone.0014002.g008

of the 21 genes were found significantly differentially expressed (p<0.05) between DM and NoDM patients in the validation set with coherent up and downregulation in the respective clinical groups. Nine additional genes showed up and downregulation in the same direction as what was found in the initial analyses compared to the initial analyses. However, these genes did not reach significant p-values in the validation set (0.05<p<0.5). The remaining 5 genes showed no difference between DM and NoDM (see Table S4).

Out of the 38 tumor associated DEGs 29 had available gene expression in the tumor-epithelial LCM validation set. Eight out of the 29 genes were found significantly differentially expressed (p<0.05) between DM and NoDM patients in the validation set with coherent up and downregulation in the respective clinical groups compared to the initial analyses. Fourteen additional genes showed up and downregulation in the same direction as what was found in the initial analyses. However, these genes did not reach significant p-values in the validation set (0.05<p<0.5). The remaining 6 genes showed no difference between DM and NoDM (one gene had non-significant opposite regulation in the validation set).

Out of the 26 overlapping DEGs 19 had available gene expression in the tumor-epithelial LCM and the tumor-stroma validation sets. Eight out of the 19 genes were found significantly differentially expressed (p<0.05) between DM and NoDM patients in the tumor-epithelial validation set. The eight genes had coherent up and downregulation in the respective clinical groups compared to the initial analyses. Six additional genes showed up and downregulation in the same direction as what was found in the initial analyses. However, these genes did not reach significant p-values in the validation set (0.05<p<0.5). The remaining 5 genes showed no difference between DM and NoDM (one gene had non-significant opposite regulation in the validation set). In the tumor-stroma validation set, one gene (ABAT) was found significantly differentially expressed (p<0.05), and was among the eight significant genes in the tumor-epithelial set. Eight genes showed up and downregulation in the same direction as what was found in the initial analyses. However, these genes did not reach significant p-values in the validation set (0.05<p<0.5). The remaining 10 genes showd no difference between DM and NoDM (one gene had non-significant opposite regulation in the tumor-stroma validation set).

Out of the five stroma ascribed genes, one gene (PIP5K2A) was found significantly differentially expressed in the tumor-stroma validation set. This gene was not significantly differentially expressed in the tumor-epithelial validation set. Thus, the PIP5K2A seem to be validated as a gene being significant differentially expressed in the tumor-stroma cells but not in tumor-epithelial cells of DM vs NoDM patients. This differentially expressed gene was also the most stroma related as it was only identified for one value of d in the tumor focused analyses (Figure 7). One gene (LRRC46) was found significantly differentially expressed in the tumor-stroma validation set but in the opposite direction of the initial analysis. The expression values of this probe had low variance in the validation set, and might not be a functional probe (Table S4).

Impact of weighing

The unweighted approach returned a list of DEGs in which there were varying numbers of false positives at any chosen FDR. When the statistics was weighed by cell type content under various assumptions of transcription levels in adipocytes and stromal cells, we identified a set of re-occurring genes that were differentially expressed between the DM and NoDM group. DEGs identified under different statistical scenarios appear more robust and are more likely true positives. However, the effect of weighing samples differently in the analyses is similar to decreasing the sample size of the dataset, since each sample count less than 1. Hence, some of the differences among the lists of DEGs could be due to a sample size effect and not the weighing it-self. The different assumptions on transcription levels in adipocytes showed a miniscule impact on the numbers of identified DEGs, and were thus set to zero, although we acknowledge that there are studies emphasizing the importance of adipocytes in breast cancer [31,32].

It should be noted that we, on the basis of weighing, can not state whether or not a gene is expressed to a higher extent in tumor epithelial cells compared to stromal cells. We merely propose to which cell type the expression *differences* (between DM and NoDM) of a gene could be ascribed or associated.

Conclusions

We present an *in silico* method for utilizing histopathological information on tissue content of tumor biopsies in the statistical calculations of differentially expression of genes in microarray data. This approach was used to identify genes significantly differentially expressed between tumors from patients who experienced distant metastasis and tumors from those who did not. The weighted analyses were utilized to ascribe and associate gene expression differences between the two patient groups to tumor epithelial and stromal cells. Although the stromal transcription contribution was measurable in data obtained from grossly dissected tumor tissue, the differences in gene expression between DM and NoDM seem mainly to be related to tumor epithelial cells, and the majority of these genes can also be identified by the unweighted bulk tumor expression. The analyses also aided in identifying a set of core genes which seems to be profoundly different in their expression patterns between the two groups, independent of the cellular constitution. Thus, genes reappearing in the weighted analyses under different assumptions of cellular contribution to the overall transcription level have a higher probability of being true findings.

Materials and Methods

Ethics statement

The study was approved by the national ethics committee (Ethical Commitee for Aarhus county) and by "Datatilsynet" (The Data Inspectorate - an independent administrative body under the The Ministry of Government Administration and Reform). Oral informed consent was mandatory, and a procedure approved by the ethical committee at that time (1982–1987).

Patient material

The 198 breast tumor samples with high quality gene expression data utilized in this study were part of 267 fresh frozen tumor samples (stored at $-80^{\circ}C$ in Denmark) available after total mastectomy surgery. The tumor samples were originally stored for the purpose of estrogen receptor staining in the Danish Breast Cancer Group 82 b and c cohort (DBCG82b&c). DBCG82 b and c studies comprise a collection of tumor tissues from 3,083 high-risk Danish breast cancer patients diagnosed in the period 1982–1990. High-risk was defined as positive lymph nodes and/or tumor size larger than 5 cm and/or invasion of tumor to surrounding skin or pectoral fascia. Total mastectomy with partial axillary dissection was performed on all women, and a median of seven lymph nodes was removed from the axilla.

Premenopausal women (DBCG b protocol) were randomized to receive radiation therapy and CMF (cyclophosphamide, methotrexate, fluorouracil; eight cycles) or only CMF chemotherapy (9 cycles) [33]

Postmenopausal women (DBCG c protocol) were randomized to receive radiation therapy+tamoxifen (30 mg daily for 1 year) or tamoxifen alone

Follow-up

Patients were followed routinely at regular intervals the first 10 years or until the first recurrence, death or new primary cancer. Recorded endpoints were locoregional recurrence (LRR), distant metastases (DM) and contralateral breast cancer (CBC) [34].

Sample handling

Fresh frozen tumor samples (approximately 5–10 mm^3) from a subset of 267 out of the 3,083 patients in the DBCG82 b and c protocols were available for this study. All tumor samples were cut in three and the centre section was used for total RNA extraction whereas the two flanking pieces were used for histopathological analyses using Haematoxylin & Eosin (HE) staining (Figure S1). Approximately 40 mg of tissue was used for total RNA extraction using the Qiagen Midi kit Extraction column procedure (Qiagen) after homogenisation using the Mixer Mill (MM301, Retsch). RNA quality was assessed using the NanoDrop instrument (concentration and purity), and the Agilent Bioanalyser instrument (degradation). Samples showing a degradation factor $>20\%$ were excluded from further analyses: the remaining 218 RNA samples of good quality were stored at $-80^{\circ}C$.

Histopathology

Haematoxylin & Eosin (HE)-stained sections were prepared from the two flanking tissue pieces facing the centre section used for RNA extraction (Figure S1), and HE sections were used for evaluating the cellular composition of the tissue sample. The tissue components evaluated were: 1) stroma, primarily comprising tumor-related stroma but also normal, surrounding stroma including vessel walls and lymphocytes. 2) epithelium, comprising tumor epithelium and possible normal epithelium entrapped in the tumor area or lying subjacent to the invasive component, and finally, 3) adipocytes entrapped in or surrounding the tumorarea. The area fractions from two sections per patient sample were estimated by a pathologist (JMN), and validated by stereological point counting [35]. A grid consisting of 20–70 points (depending on size of the tissue sample) were superimposed on each tissue section using a projection microscope and the entire section was evaluated by moving the grid in a random, systematic way. Hits on folds, not allowing proper morphological recognition of the structures, were excluded. Area fractions were calculated as number of points hitting profiles divided by total number of tissue points.

Most sections were entirely comprised of invasive tumor, and in these the amount of normal tissue stroma was negligible.

Microarray analysis

The microarray system used in the study was the Applied Biosystem Human Genome Survey Microarray version 2.0. These are whole genome arrays spotted with 32878 probes covering 29098 genes. The platform utilizes chemiluminescence labeling in a single channel system. The probes are 60-mers, mostly mapped within 1500 bases of the 3′ end of the source transcript, and were designed to match common regions of multiple alternative transcripts for a particular gene. For some genes there are multiple probes, although 87% of the genes are targeted by a single probe. In addition to the human gene probes, the microarray contains numerous internal control probes for monitoring the experimental steps in the amplification, labeling and hybridization procedure. A second set of control probes is present for intra array normalization purposes (spot to spot normalization). These probes are 20-mers printed alongside the gene-probes in every spot. The shorter control-probes are complementary to a fluorescently labeled control sequence that is added to the hybridization solution. The fluorescent signal emitted should be identical for every spot; the gene-spot signal is normalized parallel to the difference in the fluorescent signal in the same spot compared to all the other spots [36]. 500 ng of total RNA was used as input in the amplification and labeling procedure and 10 μg of labeled and amplified cRNA was hybridized onto the array for 16 hours followed by washing and signal detection. Twenty arrays were removed due to too low present call or failed out on the amplification efficiency control probes, 7 samples with no available histopathology were excluded from the weighted analyses (but included in the unweighted) giving a total of 191 unique samples with good quality expression data and histopathologic information.

Data processing and normalization

First, flagged intensities and probes with signal to noise ratio below 3 were removed from the raw data. Next, the number of probes was further reduced to 17910, by removing those that had missing values in more that 80% of the samples. The quantile normalization procedure was applied using ABarray library in R and the missing values were imputed using the k-nearest neighbors algorithm of the smida library in R. After re-scaling the expression on each array so that they sum to 1 a log2 transformation was applied. Data is accessible at NCBI GEO database accession GSE24117.

Statistical analysis

Across the whole dataset, the percentages of stroma cell area varied from 5% to 85%, for tumor cells; from 5% to 85%, and for adipocytes; from 0% to 50%. A two-sample Kolmogorov-Smirnov test was used to compare the distribution of the different cell types in the DM and NoDM groups [37].

To incorporate the information on cell type abundance into the testing procedure, the tumor-weighted or stroma-weighted mean expression of the gene was computed instead of the arithmetic mean, for both groups of patients (DM and NoDM) as $\bar{X}_{DM} = \frac{\sum_{i\in DM} w_i X_i}{\sum_{i\in DM} w_i}$ and $\overline{X}_{NoDM} = \frac{\sum_{j\in NoDM} w_j X_j}{\sum_{j\in NoDM} w_j}$ where the sums go over all samples in each cohort and the weight w_i and w_j is the mean percentage (average of the two sections per sample) of area covered by tumor (or stroma) in the sample. The difference of the means was taken and standardized giving the statistics $t_w = \frac{\bar{X}_{DM} - \bar{X}_{NoDM}}{\hat{\sigma}}$, where $\hat{\sigma} = \hat{S}_p \sqrt{\frac{\sum_{i\in DM} w_i^2}{\left(\sum_{i\in DM} w_i\right)^2} + \frac{\sum_{j\in NoDM} w_j^2}{\left(\sum_{j\in NoDM} w_j\right)^2}}$. We assumed that the variability in the gene expression in both cohorts is equal and estimated the pooled variance by $\hat{S}_p^2 = \frac{(n_{DM}-1)\hat{S}_{DM}^2 + (n_{NoDM}-1)\hat{S}_{NoDM}^2}{n_{DM}+n_{NoDM}-2}$, $\hat{S}_{DM}^2$, and $\hat{S}_{NoDM}^2$, being the estimated variances of the respective cohorts and n_{DM},n_{NoDM} their sizes. The p-values were computed by performing permutation test and after a 5% FDR adjustment for multiple testing, different sets of differentially expressed genes (DEGs) between the two cohorts were identified. The un-weighted analysis was performed by setting the weights to 1 which is equivalent the standard t-test with equal variances.

The tumor-focused and the stroma-focused analyses were carried out under various assumptions. In the first series of analyses we assumed that the total gene transcription of the three tissue components (tumor, stroma and adipocytes) occurred at an equal level. However, due to uncertainty around the transcription level of adipose tissue, the weighted analysis was repeated for various relative efficiencies ***(c)*** of transcription of adipocytes compared to tumor cells. For different values of ***c*** ranging from 0 to 1, the adipocytes percentage area ***(a)*** was scaled to ***ac*** and the percentages of area covered by tumor and stroma were re-scaled so that they summed up to 100. The re-scaled tumor ***(t')*** and stroma ***(s')*** weights were computed as $t' = t/(t+s+ac)$ and $s' = s/(t+s+ac)$, where ***t***, ***s*** and ***a*** are respectively, tumor, stromal and adipocyte cell area proportions in the original data and ***c*** the relative level of transcription of adipocytes compared to the other two tissue components.

The analyses carried out for the other selected values of *c* gave different sets of genes, differentially expressed between patients who developed distance metastasis and those who did not. In both series of analyses (tumor-weighted and stroma-weighted, for different levels of *c*), some genes seemed to be consistently differentially expressed regardless of the assumption on the level of transcription of adipocytes. Next, the level of transcription of the adipocytes was set to zero and the cell type-weighted analysis was performed under different assumptions on the level of transcription ***d*** of stroma cells compared to tumor cells. Analogous to the first series of analyses, for each level of *d* the percentages of area covered by tumor and stroma were re-scaled to sum up to 1. These new weights were computed ad $t'' = t'/(t'+s'd)$ and $s'' = (t'+s') - t''$.

Validation data

Gene expression data and associated clinical information on metastatic disease were available from microdissected tumor stroma and tumor epithelium from patients with invasive ductal carcinoma [15]. The tumor epithelial dataset included 61 patients with either distant metastatic disease (16) or no local or distant metastatic disease (45); the tumor-stroma dataset included 50 patients with either distant metastatic disease (10) or no local or distant metastatic disease (40). (Out of the 50 patients with available tumor-stroma gene expression two patients were not among the 61 with available tumor-epithelial expression data). The samples in the validation set had been analyzed on Agilent Whole Human Genome 44K arrays and hence, probes were matched between the Applied Biosystem whole genome survey microarrays and the Agilent platform by gene symbols. For genes being represented by more than one probe, the probe that matched the target RefSeqs was selected. In cases where multiple probes matched the RefSeq, the probe with highest variance across the sample cohort was selected. Out of the 99 DEGs in SACsev and TACsev combined, we were able to identify 74 matching genes in the validation set (24 out of 31 DEGs in SACsev and 69 out of 94 DEGs in TACsev) (Table S5 and S6).

Supporting Information

Figure S1 RNA extraction. Fresh-frozen tumor piece cut in three, a, b and c. Sections cut from pieces a and c for pathological estimation of area percentages of adipocytes, stromal cells and carcinoma cells. Centre piece b was used for total RNA extraction and microarray analyses.
Found at: doi:10.1371/journal.pone.0014002.s001 (0.27 MB PDF)

Table S1 Genes associated with tumor epithelial and stromal expression. List of genes (Gene symbol and Celera Gene ID) with reported cell type association in literature, were compared to the fold change (and local FDR) from a SAM analysis between the 15 samples with the highest tumor cell percentage and the 15 samples with the highest stroma cell percentage. The Pearson correlations (and p-value) for each gene to the tumor and stroma cell percentage across all 198 samples are also included.
Found at: doi:10.1371/journal.pone.0014002.s002 (0.04 MB XLS)

Table S2 UWA geneprobe list. List of DEGs from the unweighted analysis, 182 gene-probes differentially expressed in tumor samples from patients who experienced distant metastasis compared with those who did not.
Found at: doi:10.1371/journal.pone.0014002.s003 (0.04 MB XLS)

Table S3 DEGs under various assumptions of d. Lists of all DEGs found in the various weigthed analyses under different assumptions of the contribution of mRNA transcription from stroma.
Found at: doi:10.1371/journal.pone.0014002.s004 (0.10 MB XLS)

Table S4 Validated DEGs in LCM stroma and tumor epithelial expression data. List of 74 genes that were matched to the stroma and tumor epithelial expression validation set. Left columns in the split table show the original regulation of genes in DM vs. NoDM found in the stroma and tumor weighted analyses, respectively. The next column shows the regulation seen in the validation sets (only for those with a p-value<0.5). The significant differences in the validation sets are highlighted in red.

Found at: doi:10.1371/journal.pone.0014002.s005 (0.03 MB XLS)

Table S5 LCM Stroma. List of all gene probes with gene expression data for the matching 74 genes in the LCM stroma. Left column annotates no distant metastasis = 0 and metastasis = 1.
Found at: doi:10.1371/journal.pone.0014002.s006 (0.15 MB XLS)

Table S6 LCM Epi. List of all gene probes with gene expression data for the matching 74 genes in the LCM tumor epithelial. Left column annotates no distant metastasis = 0 and metastasis = 1.
Found at: doi:10.1371/journal.pone.0014002.s007 (0.18 MB XLS)

References

1. Kamangar F, Dores GM, Anderson WF (2006) Patterns of cancer incidence, mortality, and prevalence across five continents: defining priorities to reduce cancer disparities in different geographic regions of the world. J Clin Oncol 24: 2137–2150.
2. Bauer KR, Brown M, Cress RD, Parise CA, Caggiano V (2007) Descriptive analysis of estrogen receptor (ER)-negative, progesterone receptor (PR)-negative, and HER2-negative invasive breast cancer, the so-called triple-negative phenotype: a population-based study from the California cancer Registry. Cancer 109: 1721–1728.
3. Eisen MB, Brown PO (1999) DNA arrays for analysis of gene expression. Methods Enzymol 303: 179–205.
4. Perou CM, Sorlie T, Eisen MB, van de RM, Jeffrey SS, et al. (2000) Molecular portraits of human breast tumours. Nature 406: 747–752.
5. Sorlie T, Perou CM, Tibshirani R, Aas T, Geisler S, et al. (2001) Gene expression patterns of breast carcinomas distinguish tumor subclasses with clinical implications. Proc Natl Acad Sci U S A 98: 10869–10874.
6. Sorlie T, Tibshirani R, Parker J, Hastie T, Marron JS, et al. (2003) Repeated observation of breast tumor subtypes in independent gene expression data sets. Proc Natl Acad Sci U S A 100: 8418–8423.
7. van't Veer LJ, Dai H, van de Vijver MJ, He YD, Hart AA, et al. (2002) Gene expression profiling predicts clinical outcome of breast cancer. Nature 415: 530–536.
8. Cardoso F, Saghatchian M, Thompson A, Rutgers E (2008) Inconsistent criteria used in American Society of Clinical Oncology 2007 update of recommendations for the use of tumor markers in breast cancer. J Clin Oncol 26: 2058–2059.
9. Paik S, Shak S, Tang G, Kim C, Baker J, et al. (2004) A multigene assay to predict recurrence of tamoxifen-treated, node-negative breast cancer. N Engl J Med 351: 2817–2826.
10. Paik S, Tang G, Shak S, Kim C, Baker J, et al. (2006) Gene expression and benefit of chemotherapy in women with node-negative, estrogen receptor-positive breast cancer. J Clin Oncol 24: 3726–3734.
11. Sparano JA, Paik S (2008) Development of the 21-gene assay and its application in clinical practice and clinical trials. J Clin Oncol 26: 721–728.
12. van de Vijver MJ, He YD, van't Veer LJ, Dai H, Hart AA, et al. (2002) A gene-expression signature as a predictor of survival in breast cancer. N Engl J Med 347: 1999–2009.
13. Radisky D, Hagios C, Bissell MJ (2001) Tumors are unique organs defined by abnormal signaling and context. Semin Cancer Biol 11: 87–95.
14. Bissell MJ, Radisky DC, Rizki A, Weaver VM, Petersen OW (2002) The organizing principle: microenvironmental influences in the normal and malignant breast. Differentiation 70: 537–546.
15. Finak G, Bertos N, Pepin F, Sadekova S, Souleimanova M, et al. (2008) Stromal gene expression predicts clinical outcome in breast cancer. Nat Med 14: 518–527.
16. Sugiyama Y, Farrow B, Murillo C, Li J, Watanabe H, et al. (2005) Analysis of differential gene expression patterns in colon cancer and cancer stroma using microdissected tissues. Gastroenterology 128: 480–486.
17. Cleator SJ, Powles TJ, Dexter T, Fulford L, Mackay A, et al. (2006) The effect of the stromal component of breast tumours on prediction of clinical outcome using gene expression microarray analysis. Breast Cancer Res 8: R32.
18. Stuart RO, Wachsman W, Berry CC, Wang-Rodriguez J, Wasserman L, et al. (2004) In silico dissection of cell-type-associated patterns of gene expression in prostate cancer. Proc Natl Acad Sci U S A 101: 615–620.
19. Tusher VG, Tibshirani R, Chu G (2001) Significance analysis of microarrays applied to the ionizing radiation response. Proc Natl Acad Sci U S A 98: 5116–5121.

Acknowledgments

We thank Prof. Jahn Martin Nesland at Division of Pathology, Norwegian Radium Hospital, Oslo University Hospital for performing the initial histopathological evaluation of the samples.

Author Contributions

Conceived and designed the experiments: SM HM TT JA GF MP JO ALBD AF TS. Performed the experiments: SM TT GF. Analyzed the data: SM HM GF AF. Contributed reagents/materials/analysis tools: JA MP JO ALBD AF TS. Wrote the paper: SM HM TT JA JO ALBD AF TS. Performed extensive analysis of the validation data set: GF. Supplied the validation set and interpretion of results: MP.

20. Farmer P, Bonnefoi H, Anderle P, Cameron D, Wirapati P, et al. (2009) A stroma-related gene signature predicts resistance to neoadjuvant chemotherapy in breast cancer. Nat Med 15: 68–74.
21. Franzen LE, Ekstedt M, Kechagias S, Bodin L (2005) Semiquantitative evaluation overestimates the degree of steatosis in liver biopsies: a comparison to stereological point counting. Mod Pathol 18: 912–916.
22. Carter CJ (2007) Multiple genes and factors associated with bipolar disorder converge on growth factor and stress activated kinase pathways controlling translation initiation: implications for oligodendrocyte viability. Neurochem Int 50: 461–490.
23. Miller MM, James RA, Richer JK, Gordon DF, Wood WM, et al. (1997) Progesterone regulated expression of flavin-containing monooxygenase 5 by the B-isoform of progesterone receptors: implications for tamoxifen carcinogenicity. J Clin Endocrinol Metab 82: 2956–2961.
24. Blake CA, Brown LM, Duncan MW, Hunsucker SW, Helmke SM (2005) Estrogen regulation of the rat anterior pituitary gland proteome. Exp Biol Med (Maywood) 230: 800–807.
25. De Souza SE, De Bessa SA, Netto MM, Nagai MA (2008) Silencing of LRRC49 and THAP10 genes by bidirectional promoter hypermethylation is a frequent event in breast cancer. Int J Oncol 33: 25–31.
26. Sakaguchi G, Orita S, Maeda M, Igarashi H, Takai Y (1995) Molecular cloning of an isoform of Doc2 having two C2-like domains. Biochem Biophys Res Commun 217: 1053–1061.
27. Wakefield L, Robinson J, Long H, Ibbitt JC, Cooke S, et al. (2008) Arylamine N-acetyltransferase 1 expression in breast cancer cell lines: a potential marker in estrogen receptor-positive tumors. Genes Chromosomes Cancer 47: 118–126.
28. Gonda TJ, Leo P, Ramsay RG (2008) Estrogen and MYB in breast cancer: potential for new therapies. Expert Opin Biol Ther 8: 713–717.
29. Yau WL, Lung HL, Zabarovsky ER, Lerman MI, Sham JS, et al. (2006) Functional studies of the chromosome 3p21.3 candidate tumor suppressor gene BLU/ZMYND10 in nasopharyngeal carcinoma. Int J Cancer 119: 2821–2826.
30. Su LK, Qi Y (2001) Characterization of human MAPRE genes and their proteins. Genomics 71: 142–149.
31. Koda M, Sulkowska M, Kanczuga-Koda L, Jarzabek K, Sulkowski S (2007) Expression of leptin and its receptor in female breast cancer in relation with selected apoptotic markers. Folia Histochem Cytobiol 45 Suppl 1: S187–S191.
32. Tessitore L, Vizio B, Pesola D, Cecchini F, Mussa A, et al. (2004) Adipocyte expression and circulating levels of leptin increase in both gynaecological and breast cancer patients. Int J Oncol 24: 1529–1535.
33. Kyndi M, Overgaard M, Nielsen HM, Sorensen FB, Knudsen H, et al. (2009) High local recurrence risk is not associated with large survival reduction after postmastectomy radiotherapy in high-risk breast cancer: a subgroup analysis of DBCG 82 b&c. Radiother Oncol 90: 74–79.
34. Nielsen HM, Overgaard M, Grau C, Jensen AR, Overgaard J (2006) Study of failure pattern among high-risk breast cancer patients with or without postmastectomy radiotherapy in addition to adjuvant systemic therapy: long-term results from the Danish Breast Cancer Cooperative Group DBCG 82 b and c randomized studies. J Clin Oncol 24: 2268–2275.
35. Gundersen HJ, Bagger P, Bendtsen TF, Evans SM, Korbo L, et al. (1988) The new stereological tools: disector, fractionator, nucleator and point sampled intercepts and their use in pathological research and diagnosis. APMIS 96: 857–881.
36. Noth S, Benecke A (2005) Avoiding inconsistencies over time and tracking difficulties in Applied Biosystems AB1700/Panther probe-to-gene annotations. BMC Bioinformatics 6: 307.
37. Conover WJ (1999) Practical nonparametric statics. New York: Wiley.